Understanding anti-Ovarian cancer activity of selective compounds using molecular docking, pharmacophore and QSAR studies

By

Asma Abro

Department of Environmental Sciences
Faculty of Basic & Applied Sciences
International Islamic University Islamabad
2012

Understanding anti-Ovarian cancer activity of selective compounds using molecular docking, pharmacophore and QSAR studies

Supervisor

Dr. Naveeda Riaz

Assistant Professor

Co-Supervisor

Mrs. Saima Kalsoom

PhD. Scholar (QAU)

Candidate

Asma Abro

28-FBAS/MSBI/F09

Department of Environmental Sciences
Faculty of Basic & Applied Sciences
International Islamic University Islamabad

2012

Department of Environmental Sciences

International Islamic University Islamabad

Dated: _____

FINAL APPROVAL

It is certified that we have read the thesis submitted by Ms. Asma Abro and it is our judgment that this project is of sufficient standard to warrant its acceptance by the International Islamic University, Islamabad for the M.S Degree in Bioinformatics

COMMITTEE

External Examiner
Dr. Mahmood Kiani
Professor
Bioscience, CIIT, Islamabad

Internal Examiner
Dr. Shazia Erum
Asistant Professor
Department of Environmental Sciences
International Islamic University Islamabad

Supervisor
Dr. Naveeda Riaz
Assistant Professor
Department of Environmental Sciences
International Islamic University Islamabad

Co-Supervisor
Ms. Saima Kalsoom
PhD Scholar
Quaid-i-Azam University, Islamabad

Dean, FBAS
Dr. Muhammad Irfan Khan
International Islamic University, Islamabad

A thesis submitted to Department of Environmental Sciences,
International Islamic University, Islamabad as a partial
fulfillment of requirement for the award of the
degree of MS Bioinformatics

DEDICATION

To Ammi, Abbu and Uzma

DECLARATION

This is to certify that this thesis work entitled "***Understanding anti-Ovarian cancer activity of selective compounds using molecular docking, pharmacophore and QSAR studies***" which is submitted by me, is my own effort, except where acknowledged otherwise, and that the thesis is my own composition. No part of the thesis has been previously presented for any other degree.

Date: _____ Asma Abro

CONTENTS

Acknowledgements.....i

Abbreviations.....iii

List of Figures.....v

List of Tables.....vii

Abstract.....ix

1 Introduction.....1

2 Literature Review.....3

2.1 Ovarian cancer.....3

2.1.1 Molecular Genetics.....5

2.1.2 Risk Factors.....5

2.1.3 Treatment.....6

2.2 Microtubules.....8

2.3 Microtubule Stabilizers.....11

2.4 Computer-Aided Drug Designing.....15

3 Methodology.....23

3.1 Disease selection.....24

3.2 Protein Target.....24

3.3 Collection of Data.....25

3.4 Drawing of Compounds using ChemDraw.....25

3.5 Pharmacophore Generation.....31

3.6 Molecular Field Analysis.....32

3.7 Molecular Docking.....33

3.7.1 Steps of Docking.....33

3.7.2 Ligand-Protein Interactions.....34

3.7.3 Lead identification.....35

3.7.4 Analogue Designing.....35

3.8 Quantitative Structure Activity Relationship.....35

4 Results and discussions.....36

4.1 Data Set formation.....36

4.2 Rule of Five.....36

4.3 Pharmacophore Modeling.....39

4.4 Molecular Field-Based Similarity Analysis.....48

4.5 Molecular Docking.....52

4.5.1 Active Site of Tubulin.....52

4.5.2 Molecular Docking of Standard Drugs.....55

4.5.3 Molecular Docking of selected ligands.....59

4.5.3.1 Interactions of ligands with the Target Protein.....62

4.6 Lead Compound Identification.....73

4.6.1 Binding Interactions of the Lead compound.....75

4.7 Analogues of Lead Compound.....78

4.7.1 Docking and Interactions of Analogues with Target Protein.....81

4.8 Quantitative Structure Activity Relationship.....88

Conclusion & Future Enhancements.....93

References.....95

ACKNOWLEDGEMENTS

All praise and exaltation is due to Allah S.W.T., the Creator and Sustainer of all Seen and Unseen worlds. First and foremost I would like to express my gratitude and thanksgiving to Him for providing me the bounties and blessings to complete this work. I also would like to ask Him that this project would prove as tool to help in the treatment of cancer patients. Bundle of thanks to our beloved Prophet Muhammad S.A.W. who is the sole source of guidance to us. Our love for him is ever-lasting and would never end till the end of the world.

I want to thank my supervisor Dr. Naveeda Riaz for her direction, assistance, and guidance. She has taught how good experimental work is carried out.

Ms. Saima Kulsoom, my co-supervisor is thanked for her support, encouragement and technical advice in the research work. She taught us many valuable lessons regarding our research area. I am heartily thankful to her from the initial to the final level, as she enabled me to develop an understanding of the subject.

Many thanks to Pakeeza Akram, student of Department of Environmental Science International Islamic University. I must say, this work could not be accomplished without her assistance. She had always remained there whenever there was a need.

The gracious support of my dear lab fellows Mehrin, Yusra, Jawaria, Zurah, Saba, Uzma Ali, Madeeha, Ambrin, Fatima and Arshia would always be fondly remembered.

Many good friends Sumra, Hafsa, Saba, Faiza, Sheema and Zoya are thanked for their support and they will always be fondly remembered and appreciated. The work could not have been completed without the constant support of my dearest friend Uzma, who offered both practical and emotional support throughout the writing of this thesis and has remained very supportive and encouraging over the last few years. She has given me the most support when she herself didn't realize that I needed it. She is thanked for her earnest desire to see me attain my goal.

I am highly indebted to my parents, for their exceptional assistance, support, and encouragement throughout the completion of this Master of Science degree. They form the most important part of my life. After Allah (S.W.T.), they are the sole source of my being in this world. No words can ever be sufficient for the gratitude I have for my parents. The author thanks her beloved siblings who have always remained there as a constant source of joy and relaxation.

I pray to Allah (SWT) that may He bestow me with true success in all fields in both worlds and shower His blessed knowledge upon me for the betterment of all Muslims and whole Mankind.

Ameen

Asma Abro September 2011.

ABBREVATIONS

Wt	Weight
2D	Two Dimensional
3D	Three Dimensional
A°	Angstrom
Doce	Docetaxel
FDA	Food and Drug Administration
HBA	Hydrogen Bond Acceptor
HBD	Hydrogen Bond Donor
HOMO	Highest Occupied Molecular Orbital
IC_{50}	Half Maximal Inhibitory Concentration
Log P	Partition Coefficient
LUMO	Lowest Unoccupied Molecular Orbital
MOE	Molecular Orbital Environment
Mol	Molecular
MSAA	Microtubule Stabilizing Anti-mitotic Agents
PDB	Protein Data Bank
PTX	Paclitaxel
QSAR	Quantitative Structure Activity Relationship
RSQ	R^2, the square of correlation coefficient

SSR	Sum of Squares due to regression
SSE	Sum of Squares due to Error
SST	Total Sum of Squared Deviations
VMD	Visual Molecular Dynamics

LIST OF FIGURES

Figure	TITLE	Page
Figure 2.1	Crystal structure of αβ-tubulin heterodimers showing binding sites of different anticancer agents	**12**
Figure 2.2	Overall CADD process	**18**
Figure 2.3	Approaches for de novo design	**12**
Figure 3.1	Protocol for the *in silico* drug designing and development	**21**
Figure 3.2a	FDA approved drug: Docetaxel	**25**
Figure 3.2b	FDA approved drug: Paclitaxel	**25**
Figure 4.1	Docetaxel: 2D and 3D pharmacophore	**40**
Figure 4.2	Paclitaxel: 2D and 3D pharmacophore	**40**
Figure 4.3	Epothilone1: 2D and 3D pharmacophore	**40**
Figure 4.4	Dictyostatin: 2D and 3D pharmacophore	**41**
Figure 4.5	Discodermolide: 2D and 3D pharmacophore	**41**
Figure 4.6	Laulimalide: 2D and 3D pharmacophore	**41**
Figure 4.7	Eleutherobin: 2D and 3D pharmacophore	**42**
Figure 4.8	SarcodictyinB: 2D and 3D pharmacophore	**42**
Figure 4.9	Taccalonolide: 2D and 3D pharmacophore	**42**
Figure 4.10a	Superimposed ligands along with shared features	**45**
Figure 4.10b	The shared Pharmacophore with the Pharmacophore triangle	**45**
Figure 4.11a	Field alignment of template molecules	**50**

Figure 4.11b	Field alignment of all MSAAs to the template	**50**
Figure 4.12a	Hydrophobic field points (Gold)	**50**
Figure 4.12b	Van der Waals surface field points (yellow)	**50**
Figure 4.12c	Negative field points likely to interact with HBD (blue)	**50**
Figure 4.12d	Positive field points likely to interact with HBA (red)	**50**
Figure 4.13	Amino acid residues of active site of 1JFF bind with Docetaxel	**58**
Figure 4.14	Amino acid residues of active site of 1JFF bind with Paclitaxel	**58**
Figure 4.15a	Active conformation of Taccalonolide B (AA20)	**60**
Figure 4.15b	Active conformation of Epothilone (AA20)	**60**
Figure 4.16	Amino acid residues of active site of 1JFF bind with AA4 (Discodermolide)	**77**
Figure 4.17	Amino acid residues of active site of 1JFF bind with Analog1	**85**
Figure 4.18	Amino acid residues of active site of 1JFF bind with Analog2	**85**
Figure 4.19	Amino acid residues of active site of 1JFF bind with Analog3	**86**
Figure 4.20	Amino acid residues of active site of 1JFF bind with Analog4	**86**
Figure 4.21	Amino acid residues of active site of 1JFF bind with Analog5	**87**
Figure 4.22	Plot of actual and predicted IC-50 values	**93**

LIST OF TABLES

Table	TITLE	Page
Table 2.1	Classification of Ovarian tumors	**4**
Table 2.2	The costs incurring in each step in overall drug development process	**16**
Table 3.1a	Molecular structures and IC50 values of the docking data set	**27**
Table 3.1b	Molecular structures and IC50 values of the QSAR data set	**29**
Table 4.1	Lipinski's Rule of Five applied to data set	**37**
Table 4.2	Detailed analysis of rule of five in percentage form	**39**
Table 4.3	Pharmacophore features of the respective compounds	**45**
Table 4.4	Distance of the compounds incorporated to identify the general pharmacophore model	**47**
Table 4.5	Scores for top-rank template	**51**
Table 4.6	Similarity scores after alignment of MSAAs with template	**51**
Table 4.7	Active site amino acid residues	**53**
Table 4.8	Hydrogen, Ionic and hydrophobic interactions of the standard drugs	**57**
Table 4.9	The docking Data Set and their Energy Affinity Values	**61**
Table 4.10	Binding Interactions and distances of Data Set showing all the three kinds of interactions including Hydrogen Bonding,	**63**

Hydrophobic and ionic Interactions

Table 4.11 Lead compound with structure and binding interactions **74**

Table 4.12 Analogues of the lead compound along the IUPAC names and structures **79**

Table 4.13 Binding interactions of analogs **82**

Table 4.14 QSAR properties for the data set of Epothilone analogs **89**

Table 4.15 Statistical parameters and their values **92**

Table 4.16 Correlation of descriptors with activity and the percentage contribution of each descriptor to activity **92**

Table 4.17 Actual and predicted IC-50 values **93**

ABSTRACT

Microtubules have always remained a mainstay in the discussion of anti-cancer drugs. Research is being carried out since over a decade on the microtubule binding agents. The already present drugs have acquired clinical disadvantages or limitations, most importantly the acquired resistance. Microtubule stabilizing anti-mitotic agents (MSAAs) has proved important therapeutic agents for the treatment of cancer. The development of new and potent MSAAs is of both clinical and research interests. Nowadays, computational techniques such as molecular docking, pharmacophore model generation and QSAR studies are gaining rapid popularity and implementation in drug designing and discovery. Ligand based pharmacophore modelling is playing a key role for the identification of ligand features for the particular targets. A model for designing the pharmacophore onto the set of 9 compounds of seven different classes and two FDA approved standard drugs is presented. AutoDock Vina was used for docking studies of data set and the target protein used was PDB ID: 1JFF, the binding interactions of the active conformations of the ligands and the target protein have been identified by using VMD. Quantitative structure-activity relationship was established to find dependency trend in MSAAs and various molecular descriptors.

The ligand based pharmacophore model with three hydrophobic or aromatic groups, four Hydrogen bond acceptors and one Hydrogen bond donor has been identified in order to facilitate the discovery of highly potent MSAAs. Ligand Scout 3.02 has been

used to predict the pharmacophore features for MSAAs and the distances between pharmacophore features have been calculated through the software VMD. Molecular docking study was conducted in order to identify the lead compound that bind Tubulin protein. Lead compound showed strong ligand-protein interaction which includes 6 ionic bonds, 14 hydrogen bonds and 32 hydrophobic interactions and IC_{50} value 0.0065 μM and Binding energy is -10.5Kcal/mol. Five analogues of the lead compound were made. They were also docked in order to predict their bioactivity. In QSAR, Molecular descriptors were calculated and correlation was determined between IC_{50} and molar volume, molar refractivity, E_{HOMO}, E_{LUMO} and total energy. On the basis of above computational studies some new compounds were identified that act as more potent MSAAs and these new analogues have increased binding interactions.

CHAPTER 1
INTRODUCTION

1. INTRODUCTION

Ovarian cancer is the primary cause of death from gynecological cancer. It is ninth most common cancer and stands sixth in ranking out of all the cancer-related deaths in women. In 2010, in the United States, 21,880 new cases were diagnosed and 13,850 women died of ovarian cancer. In Pakistan too, it is the most fatal malignancy and the most common cancer of gynecological origin. In one of the study done in Pakistan it was the fourth prevalent cancer in the hospitals of Lahore (Parvez, 1992).

The rapid turnover of microtubules is critical for the remodeling of the cytoskeleton that occurs during cell division. Microtubules extend outward from centrosomes to form the mitotic spindle, which is responsible for the separation and distribution of chromosomes to daughter cells. Because of the central role of microtubules in mitosis, drugs that affect microtubule assembly are useful in the treatment of cancer. In this study, the research is done on microtubule stabilizing anti-mitotic agents (MSAAs) that act on Tubulin protein of microtubules or interact with it. The basic reason behind choosing this topic is that these are most widely studied area in cancer treatment. However, acquired resistance to already present anti-mitotic agents, the vascular leak problems, dose-limiting toxicities related to peripheral neuropathy (Chaudhry *et al.,* 1994; Schrijvers *et al.,* 1993) and the limited solubility of common drugs such as Docetaxel and Paclitaxel require additional impetus to the discovery of new classes of more potent anticancer drugs acting preferably by a similar mechanism of action.

Using *in silico* drug designing techniques it is hoped that novel drug for the treatment of cancers such as ovarian cancer will be developed in short time span.

Thus the hypothesis is set forth *"identify lead compound that is potential candidate as Microtubule Stabilizing Anti-mitotic agent in reduced time using in silico techniques to develop new drug focusing on drug bioavailability through the increased binding interactions."*

In the present study, a pharmacophore model is generated using the information derived from data set, as yet there is no single confined pharmacophore model identified for the Microtubule Stabilizing Anti-mitotic agents that are taken into account. Therefore it will contribute positively to the cessation of worldwide spread of cancer.

Secondly, a protocol is designed that will help in the *in-silico* drug development. This protocol incorporates pharmacophore modeling, molecular docking and quantitative structure-activity relationship (QSAR). This investigation resulted in identification of lead compound and its analogue formation having tendency to be next potential drug candidate.

2D QSAR analysis was also observed in which molecular descriptors were calculated and correlation was determined which resulted in finding relationship among certain biological activity and pharmacological descriptors.

Effectiveness of work states: Lead compound is identified which will enhance the therapeutic ability and will help to develop a potent drug for the treatment of cancers particularly ovarian cancer by increasing the binding interactions and its bioavailability.

CHAPTER 2
LITERATURE REVIEW

2. LITERATURE REVIEW

2.1 Ovarian Cancer

Ovarian cancer begins in ovaries which are the glands containing the germ cells or eggs. Ovarian cancers begin when normal cells in an ovary modify and grow uncontrollably, forming a mass called a tumor. The etiology of the disease is not very clear. Evidence is found to support the following theories: (a) continuous incessant cell division and ovarian epithelia regeneration with each ovulation providing opportunity for mutation and malignant transformation; (b) malignant transformation due to pituitary gonadotropin stimulation; and (c) exposition of the ovary to carcinogens that can travel via the vagina and fallopian tubes to the ovary (Daly and Obrams, 1998).

In the standard histological scheme (Serov *et al.,* 1973), ovarian neoplasms are categorized with regard to their derivation from coelomic surface epithelium, germ cells, and the stroma and sex cord (Kaku *et al.,* 2003). Epithelial-originated tumors account for 90% of all ovarian tumors. 6% are sex cord stromal tumors, 3% germ cell ovarian tumors and 1% is metastatic tumors (Tortolero-Luna and Mitchell, 1995). The classification of ovarian tumors as presented by Zhang and co-workers (Zhang *et al.,* 2000) is given in table 2.1.

Table 2.1: Classification of ovarian tumors

Epithelial
Serous tumor
Mucinous tumors
Brenner tumors
Endometrioid carcinomas
Clear cell carcinomas
Mixed mesodermal tumors
Germ cell
Teratomas
Benign dermoid cysts (mature cystic teratomas)
Immature teratomas
Dysgerminomas
Endodermal sinus (yolk sac) tumors
Mixed germ cell tumors
Gonadal stromal
Thecomas and fibrothecomas
Granulosa cell tumors
Sertoli cell tumors
Lipid cell tumors
Metastatic

2.1.1 Molecular Genetics

The development of ovarian cancer is thought to be a multistep process that involves accumulation of genetic changes which gradually transform normal cells to neoplastic cells. A variety of changes in genomic structure, growth factor receptors, proto-oncogenes, and tumor suppressor genes have been detected in many cases of ovarian cancer (Bast *et al.,* 1993). BRCA1 and BRCA2 are the genes mainly responsible for hereditary breast-ovarian cancer syndrome. Easton and co-workers analysed the involvement of these genes in ovarian cancer patients in detail. They found that those persons with BRCA1 germ-line mutation have a lifetime risk for ovarian cancer of 40–66%. Similarly, those with BRCA2 mutation have a lifetime risk of ovarian cancer of 10–20% (Easton *et al.,* 1993, Easton *et al.,* 1995). Over-expression of oncogenes is another important mechanism in ovarian cancer. The most frequently amplified oncogenes are: *c-myc, ras, AKT2, EFG-R (erbB1), Her-2/neu (c-erbB2), CSF-1receptor (c-fms), c-myb* etc (Berchuck, 1995; Auersperg *et al.,* 1998; Lynch *et al.,* 1998).

2.1.2 Risk Factors:

Epidemiology studies of the disease have identified certain factors that are responsible for the ovarian cancer. Age is the major contributing factor in the development of the disease. Just 2-3 cases per 100,000 are the women in their twenties while 59 cases per 100,000 in women of ages around 70 (Daly and Obrams, 1998). Race is also important, ovarian cancer occurs 50% more frequently in white women than African American women (Hankinson *et al.,*

1995). Nulliparity, family history of ovarian cancer and History of fertility drug use too are the risk factors (Hartge *et al.*, 1994, Rossing *et al.*, 1994). Different studies show that history of pelvic inflammatory disease (PID), use of talc and endocrine disorder such as low serum FSH and LH, high androstenedione and dehydroepiandrosterone levels are also associated with increased risk (Harlow *et al.*, 1992; Helzlsouer *et al.*, 1995; Risch and Howe, 1995).

2.1.3 Treatment

Surgery, radiation therapy and chemotherapy are main areas in cancer treatment. These three areas when applied together can more likely cure the cancer and minimize the damage to neighboring healthy organs and tissues. The usual treatment for advanced cancer include at first the surgical removal of the tumour and affected organs, followed and/or preceded by chemotherapy consisting of a platinum agent alone (e.g., carboplatin) or in combination with paclitaxel (Taxol). Paclitaxel acts on Tubulin, a protein of microtubules, so these are elaborated in detail in the coming section.

The oldest of all treatments is surgery. Nowadays the techniques used in surgery are quite advanced and much varied. In some cases, cancer surgery is done to completely remove the localized tumours or reduce the size of tumour to increase the effectiveness of follow-up chemotherapy or radiation therapy. It may also be done to relieve pain or to repair the deformities caused by the formerly mentioned surgical process.

In the second type, different radiation sources such as X-rays, gamma rays etc are used to kill cancer cells by destroying the molecules and affecting the cell's ability to divide by damaging their DNA. Technology advances have helped producing energy beams of high accuracy, hence, minimizing the damage to neighboring healthy cells. Two types of treatment are used – external beam radiation therapy (teletherapy) and internal therapy (brachytherapy), where a radioactive source is placed inside the body close to the tumour.

A more general and effective method of treatment is chemotherapy. In this method, the drugs will reach most parts of the body. So it is effective when cancer has already spread or for the areas which cannot be reached surgically. Oral administration of a drug may be done along with injection into muscle or into a vein or sometimes into the spinal fluid. Chemotherapy alone can provide cure to a cancer sometimes, for example, in Hodgkin's disease. The aim is designing a drug, so the focus is on chemotherapy. Here, the biological agent targeted is Tubulin protein of microtubules.

There are also available a number of newer techniques such as hormonal therapy or biological therapy. In the former, the withdrawal or administration of hormones, or the interference with their function is done for cancers that require hormones to develop. Biological therapy is known as immunotherapy where the body's immune system is stimulated to fight the abnormal cancerous cells.

2.2 Microtubules

Microtubules have always remained a mainstay in the discussion of anti-cancer drugs. We describe their structure and dynamics first and then proceed to the effects of anti-cancer drugs on them. The different classes of anti-cancer agents that are being tested experimentally are also discussed.

Microtubules are required for various cellular processes. These are the dynamic structures, which form the cytoskeleton alongside actin microfilaments and intermediate filaments. Their function alternate between forming the mitotic spindle and acting as the superstructure of the interphase cytoskeleton (Hyams and Lloyd, 1994). The highly structured arrangement of microtubules is necessary for various cellular processes.

The protein was named Tubulin. It is a heterodimer that consists of two 50 kDa sub-units namely α- and β-tubulin subunits. The genes that encode tubulin have been highly conserved throughout evolution, and even within species multiple α- and β-tubulin genes encode distinct tubulin gene products. Microtubules are formed by the organization of heterodimers of α- and β-tubulin which fold and unfold as a heterodimer complex. This folding and unfolding is supported by chaperones (Lopez-Fanarraga *et al.*, 2001). They assemble in a head-to-tail fashion into linear protofilaments which after polymerization result in the characteristic microtubule cylinder that is hollow inside (Nogales and Wang, 2006).

This final structure shows polarity such that at one end is the α-tubulin subunit exposed, this is the minus end, while at the plus end is the β-tubulin subunit exposed.

There are two sites on tubulin where GTP binds. At the β-subunit, it can be hydrolyzed while a non-hydrolyzable site is present on the α-subunit. GTP binding and hydrolysis is crucial for the stability of the microtubule polymer. The plus end in the final structure is more dynamic where GTP binds to β-tubulin. This binding is required for the assembly into microtubules, after which GDP is formed by the irreversible hydrolysis of GTP. Hence, much of β-tubulin in the microtubule fiber is in the GDP-bound form with capping of GTP-bound β-tubulin at the plus end. The exposed GDP-β-tubulin before the capping leads to a conformational change, microtubule catastrophe, which is the rapid microtubule depolymerization. The fast lengthening and shortening process at the microtubule plus end is termed as dynamic instability (Mitchison and kirschner, 1984). Whereas treadmilling is another phenomenon in microtubule mechanisms where controlled loss of microtubules happens from the minus end and at the plus end gain of tubulin subunits occurs. There is no net change in microtubule mass (Risinger *et al.*, 2009).

Microtubules play a critical role in a variety of cellular processes including cell division, cell motility, intracellular trafficking, and cell shaping. The dynamic property of microtubule largely dictates the assembly of the mitotic spindle, the attachment of chromosomes to spindle microtubules, and the movement of chromosomes along the spindle. During different phases of the cell cycle, their behavior is quite dynamic. Cell cycle arrest is the result of inhibition of the microtubule assembly dynamics which leads to apoptosis (Haydn *et al.*, 1990; Zhai *et al.*, 1996; Rusan *et al.*, 2001; Checchi *et al.*, 2003); thus, proving them as significant drug targets for treating numerous diseases such as cancer. The genetic material which is present in the form of chromosomes is divided

equally between two new daughter cells. When mitotic phase occurs, the cytoskeletal microtubule network is separated apart and a bipolar spindle shaped array of microtubules is assembled outwards from the centrosome. Microtubules from the spindle become attached to the chromosomes and move them to the two spindle poles. Microtubule growing and shortening dynamics are relatively slow in interphase cells. However, When cells enter mitosis the rate of growing and shortening increases 20 to 100-fold. These extremely rapid dynamics, which are highly sensitive to modulation by antimitotic drugs, appear to be crucial in the complex movements of the chromosomes (Wilson and Jordan, 1995).

Almost invariably antimitotic agents have been found to interact specifically with tubulin, rather than with other components of the microtubule (generically referred to as "microtubule-associated proteins" or MAPS) or other proteins involved in mitosis. While antimitotic agents have significant roles in the treatment of inflammatory (colchicine), fungal (griseofulvin), and parasitic (benzimidazole carbamates) diseases, the greatest current interest in these compounds derives from their role in the treatment of cancer (Hamel, 1996).

A diverse range of structurally dissimilar antimicrotubule agents are now used as anticancer drugs (Jordan and Wilson, 2004). Microtubule drugs are generally classified as polymerizing agents or depolymerizing agents on the basis of their effects on microtubule assembly. The polymerizing agents stabilize microtubules by promoting microtubule assembly. Examples include paclitaxel and docetaxel. The depolymerizing class of agents depolymerizes microtubules by inhibiting microtubule assembly both in vitro and in vivo.

Most of these agents either bind to the colchicine or vinblastine binding site on tubulin (Singh *et al.*, 2008). The polymerization or depolymerization prevents the formation of the mitotic spindle and thence these compounds behave as antimitotic agents. Although anti-mitotic agents have earned great clinical success in chemotherapy, still there are some important drawbacks associated with their use, among these most important are innate and acquired drug resistance. As a result, new agents targeting microtubule dynamics are continually being hunted out.

In this study, polymerizing agents (microtubule stabilizers) were chosen as a subject of scrutiny. In this research work, formerly described compounds are tested using a different methodology and the most potent compound is screened out. The results may be the verification of previous researches or suggestion of new compounds.

2.3 Microtubule Stabilizers

Microtubule stabilizers mostly bind to the Taxane–binding site on Tubulin protein. The taxanes are polymerizing class of agents which bind to microtubules within the lumen of the microtubule. The β-tubulin ends with GDP-caps are stabilized by straightening them into a more stable conformation that resembles GTP-capped structure (Elie-Caille *et al.*, 2007). A shift in equilibrium results due to Taxane binding, from the soluble to polymerized forms, this will result in interphase microtubule bundling. At lower concentrations they decrease microtubule dynamicity, and this is similar to the mechanism of microtubule destabilizing agents, resulting in abnormal mitotic spindle formation, mitotic arrest and beginning of apoptosis.

Microtubule stabilizing agents have been studied extensively in the past. Most important agents, apart from the drugs Paclitaxel and Docetaxel, include the natural products such as epothilones both A and B, Discodermolide, Dictyostatin, Eleutherobin, Sarcodictyin, Laulimalide and recently revealed Taccalonolide. They bind to the Tubulin protein at Paclitaxel-binding site. All of these are included in this research work. Here we start with the brief overview of the standard drugs and each compound.

Paclitaxel is a common drug that binds to this site and thus sometimes this site is referred as Paclitaxel-binding site. Paclitaxel is a plant product isolated from Taxus brevifolia. It is widely used in the treatment of various cancers such as breast cancer, ovarian cancer and lung cancer. Paclitaxel binding site on tubulin is well characterized. It binds in a deep hydrophobic pocket on the inner surface of the microtubules (Fig 2.1) (Nogales *et al.*, 1995).

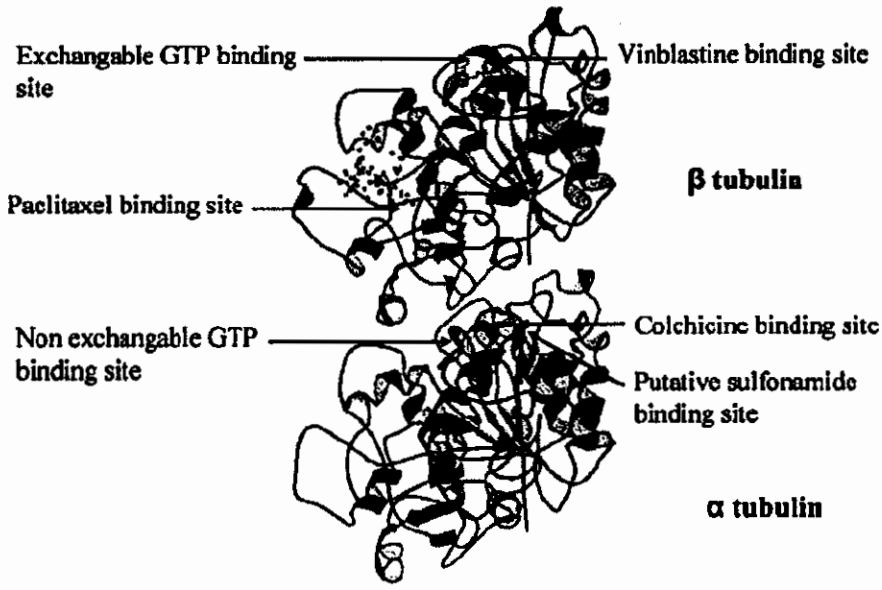

Figure 2.1: Crystal structure of αβ-tubulin heterodimers showing binding sites of different anticancer agents

It binds directly to Tubulin along the length of Microtubule (Parness and horwitz, 1981; Wilson and Jordan, 1994; George *et al.,* 1995). Paclitaxel suppresses the growing and shortening dynamics of individual microtubules of tumor cells in culture (Jordan and Wilson, 2004).

Docetaxel is the semi-synthetic analog of Paclitaxel. It is synthesized from a naturally occurring precursor, 10-deacetylbaccatin III, taken from the needles of a European yew, Taxus bacca,. Both of the drugs have earned large success in the field of chemotherapy for the treatment of solid tumors including the ovarian cancer. However, toxicities of immunosuppression and peripheral neuropathy have become the major limitations to the use of this drug. Moreover, acquired drug resistance is another problem (Risinger *et al.,* 2009).

Epothilones were isolated first in 1995 from the anti-fungal fermentation products of myxobacterium Sorangium cellulosum by Bollag and collaborators. After initial screening, they came to know that the crude extract contained some microtubule-stabilizing component. They indicated that this cytotoxic activity was related to the mitotic arrest, disorganization of cytoskeleton and the emergence of microtubule bundles in those cells treated with the drug. They discovered that epothilones stimulated microtubule assembly *in vitro* from Tubulin in a concentration-dependent manner in the absence of GTP much like the drug Paclitaxel. They compete with Paclitaxel for binding on Tubulin (Bergstralh and Ting, 2006). Epothilones are easier both to produce and work with because of their bacterial origin. Chemical syntheses of these molecules and their

analogs, may it be total or partial, allows for modification to enhance their efficacy (Mani *et al.*, 2004).

On the basis of immunosuppresive activity, Gunasekera and co-workers isolated Discodermolide from the marine sponge *Discodermia dissoluta*. In studies with purified tubulin, under various reaction conditions such as low temperatures, without MAPs, without GTP; discodermolide was found to be more potent than paclitaxel in inducing polymerization (Hamel, 1996).

Dictyostatin-1 was derived from a Republic of Maldives marine sponge in the genus *Spongia* sp. It is reported to strongly inhibit the growth of a selection of cell lines (Pettit and Cichacz, 1995). The mechanism of its cytotoxic activity is similar to that of Paclitaxel (Isbrucker et al., 2003).

Laulimalide and isolaulimalide are natural products of the marine sponge *Cacospongia mycofijiensis* with strong Taxol-like activity (Mooberry *et al.*, 1999).

The marine diterpenoids sarcodictyins A and B and eleutherobin, extracted in minute quantities from the soft corals *Sarcodictyon roseum and Eleutherobia albiflora,* have shown outstanding biological activity. Both eleutherobin and sarcodictyins show potent *in vitro* cytotoxicity against diverse tumor cell lines and compete with paclitaxel for its binding at the microtubules, inhibiting their depolymerisation (Ceccarelli *et al.*, 1999).

The taccalonolides, natural steroids derived from plants, are novel microtubule stabilizers. Their effects are same as the taxanes, including interphase microtubule bundling and mitotic arrest with multiple aberrant spindles.

2.4 Computer-Aided Drug Designing

In the field of drug design, both computational and experimental approaches are used and present complementary approaches. Nowadays, computational techniques are gaining rapid popularity and implementation in drug designing and discovery. Computer-aided drug design (CADD), computer aided molecular modeling (CAMM), computer-aided molecular design (CAMD), computer-aided rational drug design, computational drug design, *in silico* drug design and rational drug design are the different terms applied to this area.

Molecular simulations play different roles in different disciplines of science in various research areas. In bioinformatics and drug designing, the focus is on two parallel areas. First, the use of current mathematical algorithms in the field of molecular biology. Examples include simulating protein-protein interactions or protein-ligand interactions. The results are then used for further experimentation. The second approach obviously is the focus on designing new algorithms with much effective outcomes (Huang *et al.*, 2010).

The process of drug development is demanding, time consuming, costly, and requires many aspects to be considered. According to a study, the cost ranges from $800 million to $1.8 billion in the drug discovery process (Hileman, 2006). However,

depending on the type and nature of the disease being targeted and the drug, considerable variation is seen both in time and cost. Bharath and co-workers summarized the overall drug development process and the cost incurring at each step (Bharath *et al.*, 2011).

Table 2.2: the costs incurring in each step in overall drug development process

	Cost US $ Million	Cost %	Time in years
Biology			
Target identification	165	18.8	1.0
Target validation	205	23.3	2.0
Chemistry			
Screening	40	4.5	4.5
Optimization	120	13.6	2.7
Development			
Pre-clinical	90	10.2	1.6
Clinical	260	29.5	7.0
Total	880	100.0	14.7

Furthermore, out of 40,000 compounds tested in animals only 5 reach human testing and the number of compounds which is approved for reaching clinical studies is just 1 out of 5. This depicts a huge investment in terms of time, money and other resources (Kapetanovic, 2008). A report suggests that extensive usage of bioinformatics and *in silico* technologies would cause reduction up to 50% in the overall drug development cost (PricewaterhouseCoopers, 2007). Our work is all *in silico* and it suggests a new drug for the treatment of cancers in general and ovarian cancer in particular.

Application areas where CADD technologies work are two: structure based drug design and ligand based drug design. In structure-based drug design, we should have complete knowledge of the target protein structure and its active sites for finding the binding pocket, the binding energy and the steric properties of ligand and protein. It includes de novo ligand design and docking among other topics. While in ligand-based drug design, focus is on ligands which interact with the target protein. The technologies

include pharmacophore, QSAR and 3D-QSAR. Both the techniques produce lead compound as a final product. CADD process flowchart is given as drawn by Huang and collaborators in their review about CADD.

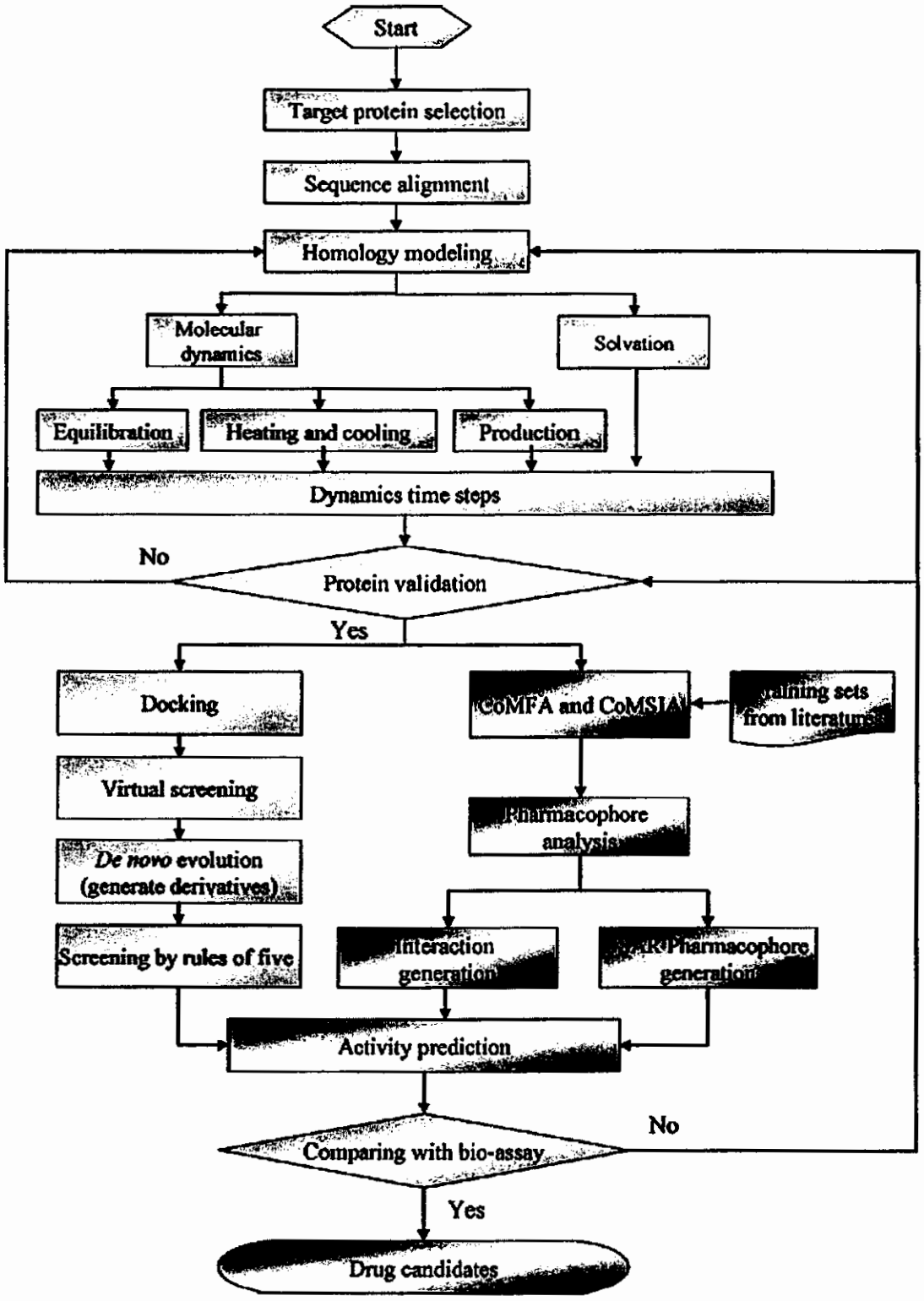

Figure 2.2: Overall CADD process

In structure based drug design, we require a protein structure at hand. Two physical methods of obtaining structure are NMR spectroscopy and X-ray diffraction. Numerous protein structures are found at RCSB PDB. Those that are not included in the PDB database can be modeled. Homology Modelling is a technique used to predict unknown protein structure by sequence similarity to known protein structure(s). If the protein sequence has 30% similarity with its template (homologous protein), it can be modeled (Marti-Renom *et al.*, 2000). *Ab initio* modeling and threading are other two methods for protein structure prediction.

Docking is a technique where non-covalent binding of a protein (receptor) and a ligand is efficiently predicted. The binding affinity with each other is also predicted. This information is used in screening virtual libraries to obtain novel bioactive compounds for future drug development.

PROLEADS (Murray *et al.*, 1999), GOLD (Jones *et al.*, 1995), AutoDock (Morris *et al.*, 1998), AutoDock Vina (Trott and Olson, 2010), DOCK 4.0 (Ewing and Kuntz, 1999), FlexX (Rarey *et al.*, 1996), CDOCKER (Wu *et al.*, 2003), LigandFit and Surflex are among the most well-known docking programs.

For producing ligands for a target protein that optimally fits into the binding site and that prove to be potentially useful, de novo ligand designing is used. In this method, fragments are positioned on the target protein in its binding cleft and these are then 'grown' to fill the available space by the optimization of van der waals, electrostatic and hydrogen bonding interactions (Congreve *et al.*, 2005).

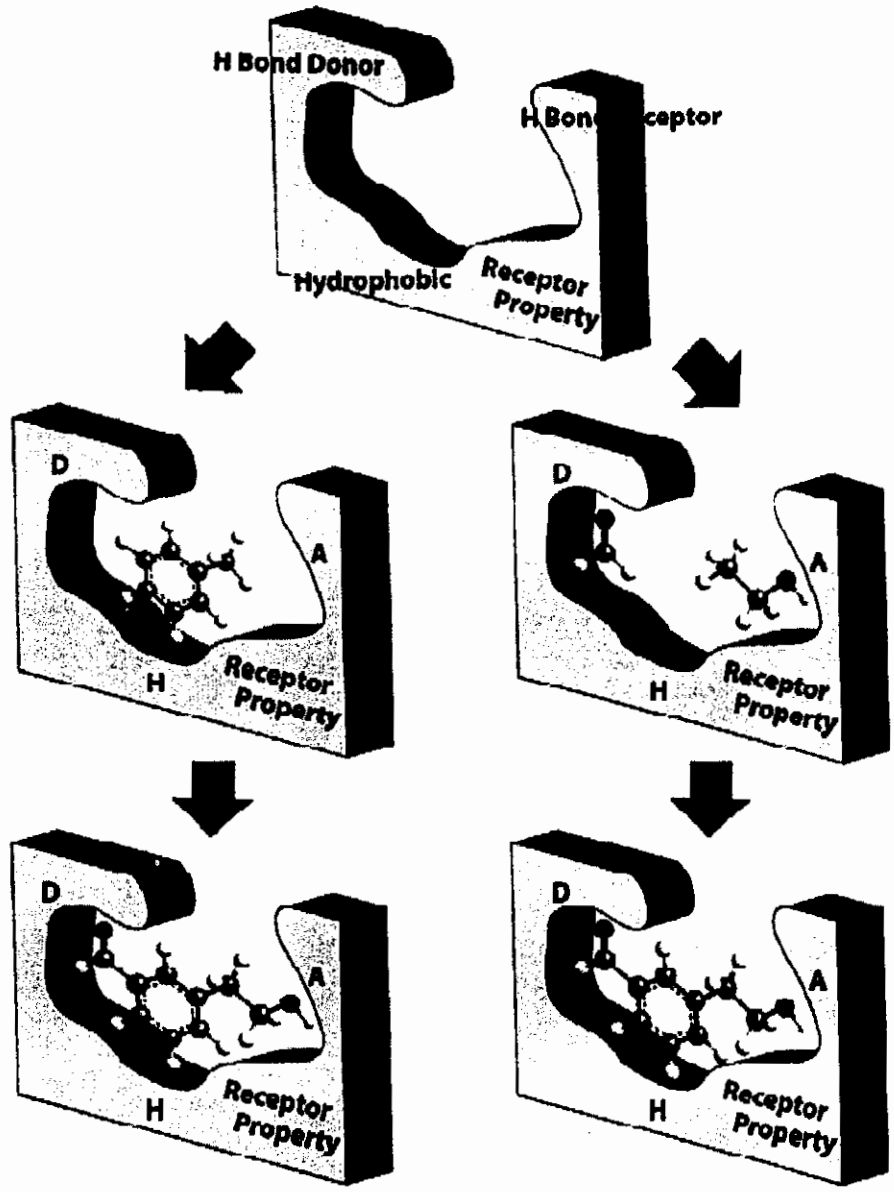

Figure 2.3: Two main approaches for de novo design (Huang *et al.*, 2010)

Ligand based techniques are used when the structure of the receptor (target protein) is not known or it cannot be predicted through modeling. Statistical techniques are used for the correlation of the structural information to Ligand activity (Singer and William, 1967).

A Pharmacophore includes aromatic rings, hydrophobic groups of compounds, hydrogen bond acceptors and donors that bind to a particular biological target plus the positive and negative ionizable groups. The Pharmacophore model is a proposed model on the 3D arrangement of such groups. Search can be performed in large databases once a model is proposed. This will lead to a significant enhancement in the number of active analogs. This has paved a way to the discovery of new bioactive compounds and in other words, lead compounds (Taft *et al.,* 2008).

During the past decades, QSAR methods especially 3D-QSAR approaches, have been successfully employed to assist the design of new drug candidates, ranging from enzyme inhibitors to receptor ligands (Chou, 2010; Trossini *et al.,* 2011; Gonzalez-Diaz *et al.,* 2010). Furthermore, they have been extensively applied in connection to medicinal chemistry research as well as proteomics, metabolomics, and bioinformatics (Prado-Prado *et al.,* 2009; Perez-Montoto, 2009). QSAR provides a correlation between the structure of ligands and the corresponding effects they produce by employing statistical and analytical tools. The descriptors characterize steric, topologic, electronic, geometric and hydrophobic properties. A common 2D QSAR method is Hansch analysis (Hansch, 1969). However, recently 3D QSAR methods are adapted such as CoMFA and CoMSIA. In CoMFA, biological activity is correlated to molecular properties through calculation of steric, electrostatic and lipophylic potentials around the Ligand molecules. Partial least

square method is then applied to the data set (Taft *et al.*, 2008). CoMSIA is more recent technology and is an extension of CoMFA. It includes additional field properties such as hydrophobic, hydrogen bond donor and acceptor.

Molecular dynamics (MD) simulation is one of the important tools in the theoretical study of biological molecules. Because molecular systems generally contain a large number of particles, it is impossible to analyze such complex systems. By using numerical methods, molecular dynamics simulation can avoid such analytic intractability. During simulation, atoms and molecules are allowed to interact for a period of time. The motion for every atom is calculated and can be played to examine the overall behavior (Mccammon et al., 1977). Overall, the background algorithm for a MD simulation includes: (1) the determination of the initial positions and velocities of every atom; (2) the calculation of forces applied on the investigated atom using inter-atomic potentials; (3) the progression of atomic positions and velocities through a short- time period. These new positions and velocities are then turned into new inputs to step 2, and when steps 2 and 3 are repeated, each repetition forms an additional time step.

CHAPTER 3
METHODOLOGY

3. METHODOLOGY

The Protocol we followed for the identification of lead compound for the treatment of ovarian cancer is summarized in the figure 3.1.

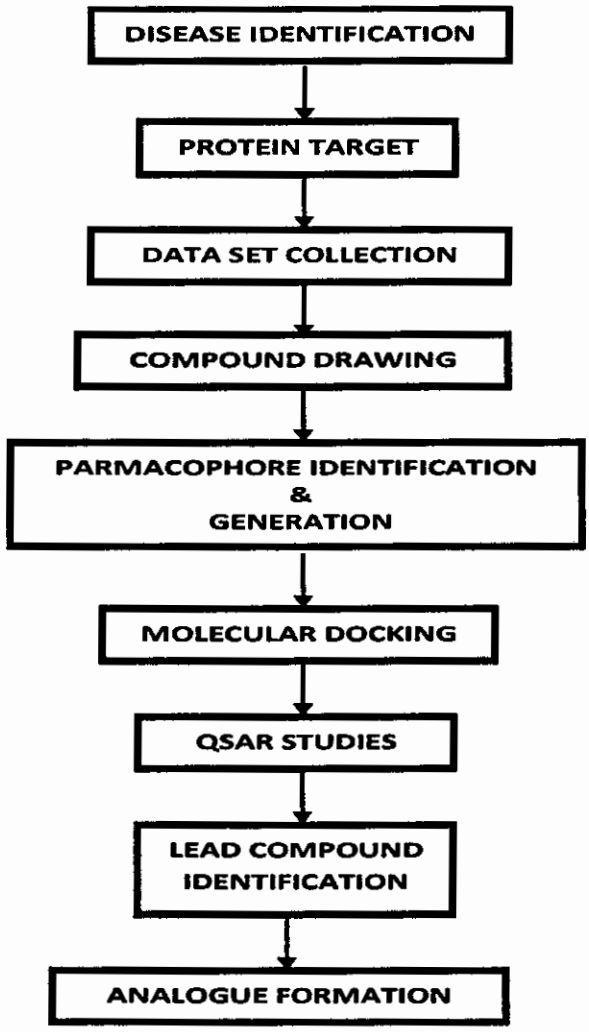

Figure 3.1: Protocol for the *in silico* drug designing and development

As the pioneer step disease was identified leading to the potential protein target. Further data was collected through a peer literature survey; it was followed by drawing of compounds in a 2D view format. Pharmacophore identification and generation was done next which was followed by QSAR analysis. The docking of compounds was the next step which resulted in the lead compound identification and analogues formations. Each step of the protocol is described below in detail along with the tools used for the accomplishment of the particular task.

3.1 Disease Selection

Mainly focus is kept on cancers in general and particularly the ovarian cancer. It is widely spreading day by day among women in spite of improvement of conditions in health sector, especially of child and mother.

3.2 Protein Target

Basically, for targeting the disease, there are two main protein targets. One, the drugs are made that effect the signaling pathway and act as Tyrosine Kinase Receptor (TKR) inhibitors that effect EGFR. Second, those that target microtubule dynamics and act on Tubulin protein. Of the second category too, there are two divisions; those that stabilize microtubules and those that destabilize microtubules. A number of crystallographic structures of tubulin depending on how it is found within several Microtubule-like conformations are now available from the RCSB Protein Data Bank (PDB) (Nogales *et al.,* 1995; Li *et al.,* 2002; Wang and Nogales, 2005). Huzil *et al.,* in 2007, while presenting the role of beta-tubulin mutations reviewed a number of tubulin

proteins and tubulin binding sites. Tubulin with pdb ID 1JFF is selected as a receptor after a thorough analysis.

3.3 Collection of Data of Ligands

Different anti-cancer microtubule stabilizing anti-mitotic agents (MSAA) considered as ligands have been selected for this study. Three standard FDA approved drugs with similar activity have been selected as reference agents (Nicolaou *et al.*, 1998; Nicolaou *et al.*, 1999; Martello *et al.*, 2001; Nicolaou *et al.*, 2003; Paterson *et al.*, 2005; Paterson *et al.*, 2007; Risinger and Mooberry, 2010). Their structures are given in figure 3.2a and 3.2b.

3.4 Drawing of Compounds Using ChemDraw

The mentioned 44 structures plus the standard drugs are all drawn using ChemDraw Ultra 8.0 (Mills, 2006). The compounds were drawn and saved in cdx format, then converted to pdb format through Chem3D Ultra 8.0. These are shown in Table 3.1a and 3.1b.

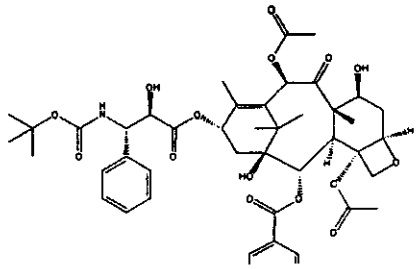

Figure 3.2a FDA approved drug: Docetaxel

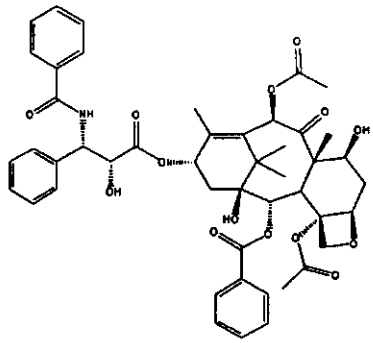

Figure 3.2b FDA approved drug: Paclitaxel

Table 3.1a: Molecular structures and IC50 values of the docking dataset:

S. No.	Structure	IC50 (μM)	S. No.	Structure	IC50 (μM)
AA1	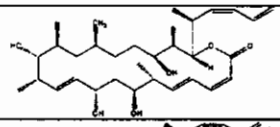	0.0098	AA2	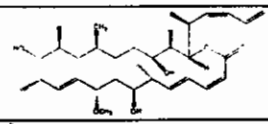	1.5
AA3	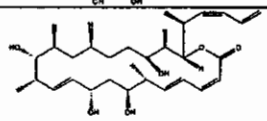	0.0082	AA4	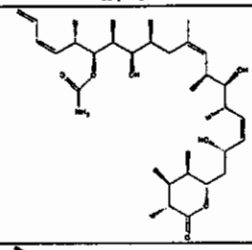	0.0065
AA5	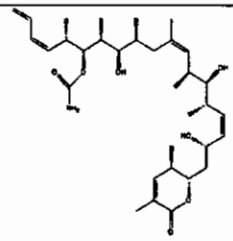	0.0061	AA6	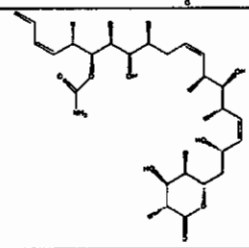	0.022
AA7	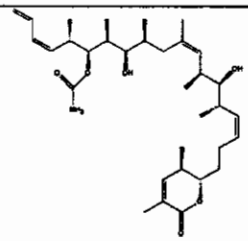	0.0065	AA8	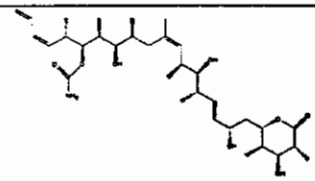	0.035
AA9	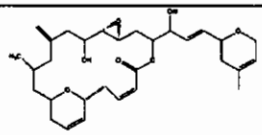	0.026	AA10	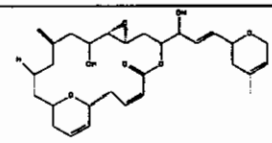	0.028
AA11	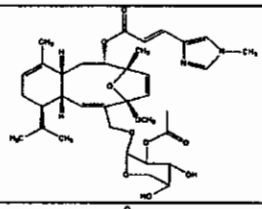	0.04	AA12	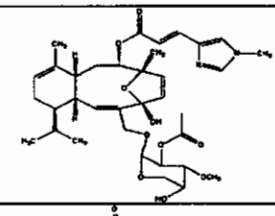	0.034
AA13	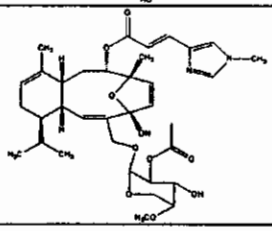	0.022	AA14	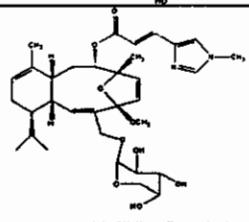	0.04

AA15	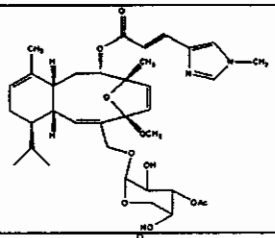	0.05	AA16	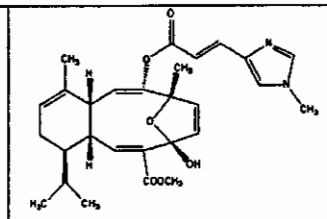	0.3
AA17	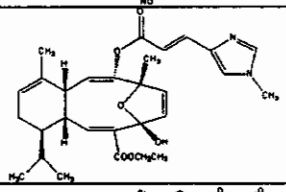	0.3	AA18	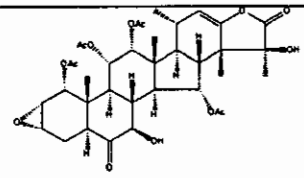	0.622
AA19	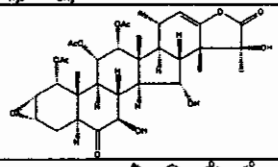	0.208	AA20	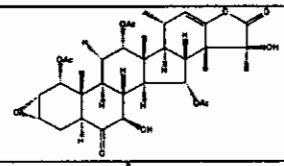	0.708
AA21	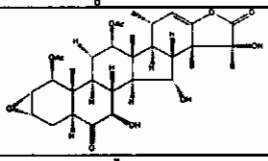	0.201	AA22	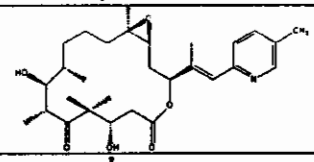	0.0003
AA23	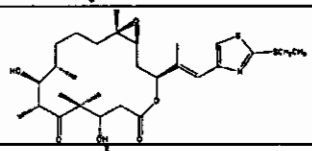	0.0035	QAA1	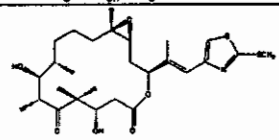	0.00017
QAA2	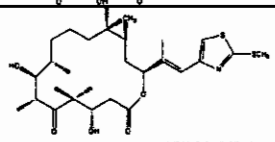	0.0001	QAA3	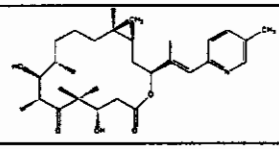	0.0003

Table 3.1b: Molecular structures and IC50 values of the QSAR data set

QAA4	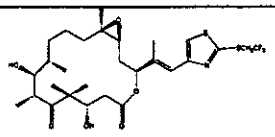	0.0035	QAA5	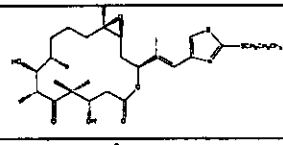	0.0044
QAA6	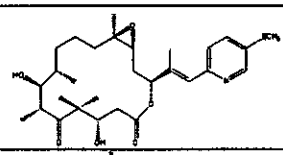	0.0004	QAA7	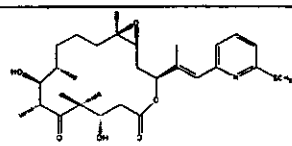	0.0033
QAA8	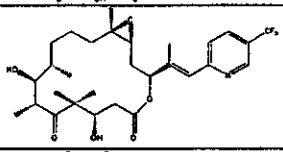	0.0043	QAA9	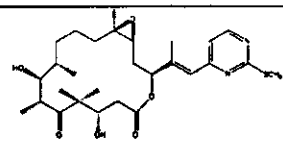	0.0086
QAA10	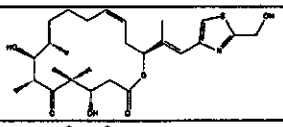	>0.1	QAA11	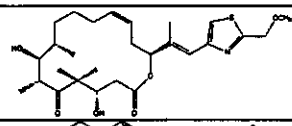	0.05
QAA12	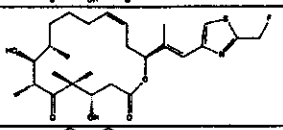	>0.1	QAA13	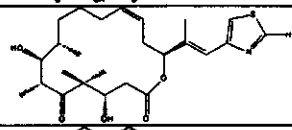	>0.1
QAA14	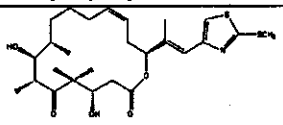	0.022	QAA15	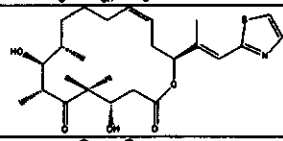	0.01
QAA16	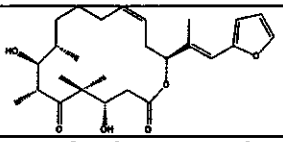	>0.1	QAA17	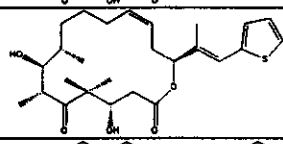	>0.1
QAA18	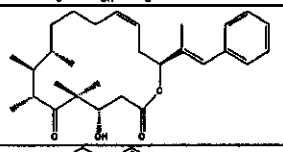	>0.1	QAA19	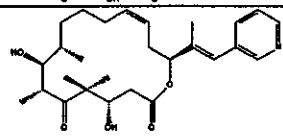	>0.1
QAA20	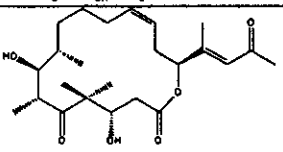	>0.1	QAA21	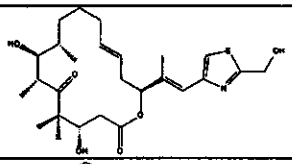	>0.1
QAA22	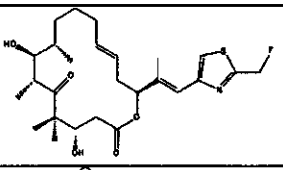	>0.1	QAA23	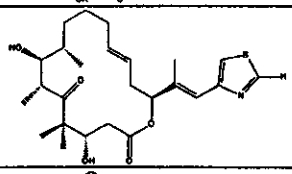	0.02
QAA24	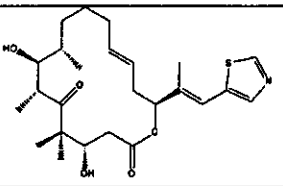	>0.1	QAA25	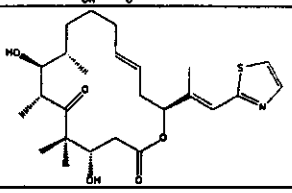	>0.1

TH-8579

QAA26	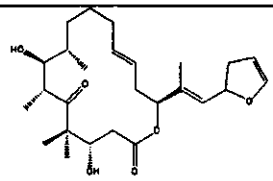	>0.1	QAA27	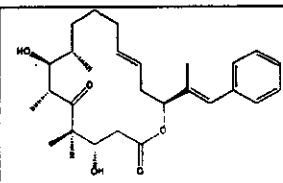	>0.1
QAA28	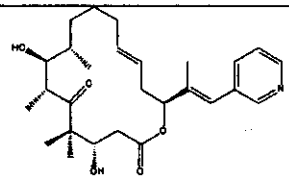	>0.1	QAA29	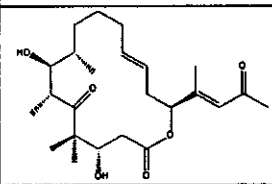	>0.1
QAA30	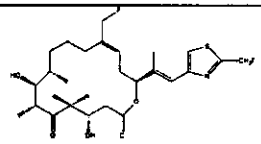	0.08	QAA31	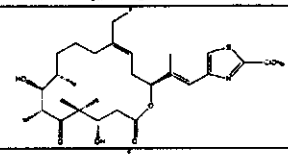	0.01
QAA32	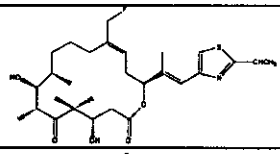	0.0012	QAA33	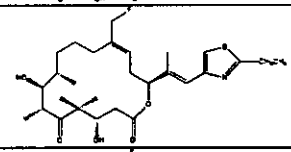	0.002
QAA34	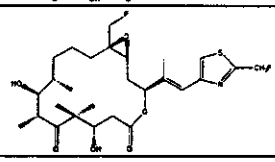	0.00054	QAA35	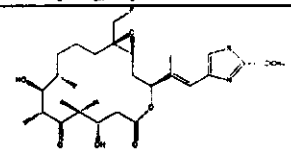	0.0004

3.5 Pharmacophore Generation

The pharmacophoric features of individual compounds as well as the pharmacophore shared between the compounds were generated using LigandScout (inte:ligand). The version used is 3.02. LigandScout is a powerful structure-based and ligand-based pharmacophore generator based on sophisticated algorithms for performing alignments and interpreting and customizing ligand-molecule interactions. The generation of shared feature pharmacophore is a powerful tool to combine the knowledge gained from multiple pharmacophores. It uses the alignment algorithm for this purpose. Alignment is done for every set of overlapping features and results in a shared feature pharmacophore.

The inputs to LigandScout were pdb files which were obtained through ChemOffice. A pdb file was opened and its pharmacophore generated. The pharmacophore and ligand were copied to alignment view through data exchange widget. This was repeated for all the ligand from each class and also for the two standard drugs. LigandScout has the additional capability of generating both 2D and 3D views. After pharmacophore generation, alignment tab was clicked. Next, the pharmacophores were selected and 'Create shared pharmacophore' button was clicked. This was set as reference and the ligands were selected and aligned to this pharmacophore. Thus a pharmacophore was generated.

3.6 Molecular Field Analysis

FieldTemplater compares molecules using their electrostatic and hydrophobic fields for finding common patterns. When applied to several molecules with different structures but having common activity, FieldTemplater determines the bioactive conformations and relative alignments of these molecules without requiring any receptor or binding site information. FieldTemplater provide a full picture of how the active molecules bind, which features they use, what shape they are, and how different series can be compared. Fields summarize the most important binding regions of a molecule and can be used both to visually compare fields of two molecules and to accurately determine the overall similarity of the fields of two different molecules. Common fields FieldTemplater works with are positive and negative electrostatic fields, van der Waals effects and hydrophobic effects on and near the surface of a molecule. Molecules which bind to a common active site tend to make similar interactions with the receptor and hence have highly similar field point patterns. FieldTemplater thus searches for common field patterns across the explored conformational space of a set of ligands looking for commonality.

Three most active ligands along with two standards were given as input to the FieldTemplater. These were processed by the software and a template was generated. This template was then used as reference for the alignment of further representative ligands of remaining MSAA classes using FieldAlign. Thus a common template was found which tells the field points common in all structurally-distinct ligands against ovarian cancer.

3.7 Molecular Docking

For performing the docking studies, tubulin protein was used. The pdb model used includes residues beta: 2-437. The actual model had residues alpha: 2-34, alpha: 61-439, one molecule of GTP, one of GDP, and one of taxol, as well as one magnesium ion at the non-exchangeable nucleotide site, and one putative zinc ion near the M-loop in the alpha-tubulin subunit along with the beta residues but these were removed as the binding site of microtubule stabilizing anti-mitotic agents is located on the beta chain. Docking was performed with AUTODOCK vina (Trott and Olson, 2010). However PDBQT files needed for docking were generated through ADT-1.5.2 (AutoDockTools) (Morris *et al.*, 2009).

3.7.1 Steps of Docking

ADT uses PDB format for the receptors and ligands for input. These were obtained through ChemOffice as described. The receptor (protein) file was opened in ADT and checked for missing atoms. These were repaired and hydrogens added. The protein was saved as RH.pdb. Next the ligand was opened. ADT automatically computes Gasteiger charges, merges non-polar hydrogens, and assigns Autodock Type to each atom. Torsions were defined which include three things: first, the root was detected. Second, torsions were chosen and rotatable bonds were converted to non-rotatable bonds and vice versa. Third, the number of torsions was set to 'most atoms'. The ligand is now ready and saved as L.pdbqt.

As rigid docking is done, macromolecule i.e., RH.pdb was employed where charges were added automatically and Hydrogens merged. This was saved as RH.pdbqt. both Receptor and ligand pdbqts are now ready. An additional step is performed of defining search grid. In this step, grid parameter file is prepared and grid properties are set. These properties were afterward used in the configuration file for docking as needed by Autodock Vina.

AutoDock Vina is a new open-source program for drug discovery and molecular docking. It offers multi-core capability, high performance, speed and ease of use (Trott and Olson, 2010). Vina uses the PDBQT molecular structure files provided in the configuration file with the extension '.conf' along with the grid parameters that include the grid points and grid box centers. The Receptor, ligand and configuration file were all put in the same directory. The out file and log file will also be generated in the same directory.

The out file contained 9 energy models with the lowest energy model being on the top. This was selected and appended at the end of original protein file, hence docked file obtained.

3.7.2 Ligand-Protein Interactions

For the interpretation of docking results, we need to find the interactions between active site of the protein and ligands. Usually three types of interactions are studied; Hydrogen, Ionic and Hydrophobic. These were studied using Visual Molecular Dynamics (VMD) computer program. Those interactions with the distance less than 4Å were kept.

3.7.3 Lead Identification

After finding Interactions, most active compound or lead was identified. This was done on the basis of three things viz. Number of interactions, most importantly Hydrogen and ionic, IC-50 values, Energy values of the model generated through docking

3.7.4 Analogue Designing

After selection of leads, analogues are designed by introducing or removing different functional groups from the lead compound.

3.8 Quantitative Structure Activity Relationship

Quantitative Structure Activity Relationship was performed for 35 ligands of one class by calculating electronic and steric descriptors. ChemDraw from ChemOffice and HyperChem Professional 8.0 (HyperCube, Inc.) were used for the calculation of these descriptors. Computational methods include molecular mechanics, molecular dynamics, and semi-empirical and ab-initio molecular orbital methods, as well as density functional theory. It is applicable to macromolecules as well as small molecules. QSAR equation was calculated alongwith different statistical parameters. In the end, values for IC-50 value are predicted and a graph is plotted between actual and predicted IC-50 values.

CHAPTER 4

RESULTS AND DISCUSSIONS

4. RESULTS AND DISCUSSION

4.1 Data Set Formation

Major representing classes of microtubule stabilizing anti-mitotic agents are taken into account for this research and analysis. It involved seven classes and each class comprising two to four analogs, making the total of 26 compounds in the data set. The data set additionally contained 2 FDA Approved drugs which were taken as standard drugs. These are Paclitaxel and Docetaxel (Wani *et al.,* 1971; Guenard *et al.,* 1993). The compounds belong to following classes: Dictyostatin, Discodermolide, Epothilone, Laulimalide, Sarcodictyin, Eleutherobin and somewhat recently discovered Taccalonolide (Nicolaou *et al.,* 1998; Nicolaou *et al.,* 1999; Martello *et al.,* 2001; Nicolaou *et al.,* 2003; Paterson *et al.,* 2005; Paterson *et al.,* 2007; Risinger and Mooberry, 2010).

4.2 Rule of Five

Although all the drugs have undergone the bioassay, Lipinski's rule of five was applied to counter check their drug-likeness properties and to incorporate the pharmacokinetics of the drug. The results are given in Table 4.1.

Table 4.1: Lipinski's rule of five applied to complete data set

ID.	HBD	HBA	LogP	Mol. Wt.
Doce	5	11	14.05	849.92
PTX	6	12	14.80	853.91
AA1	4	5	5.56	532.75
AA2	3	5	5.23	546.78
AA3	4	5	5.92	518.73
AA4	4	7	5.79	591.82
AA5	3	6	5.22	575.78
AA6	5	8	4.24	579.77
AA7	3	5	6.35	559.78
AA8	5	8	4.42	593.79
AA9	2	6	2.54	514.65
AA10	2	6	2.21	500.62
AA11	1	10	7.93	670.87
AA12	1	8	7.93	664.83
AA13	1	9	7.93	664.83
AA14	3	9	2.24	614.73
AA15	1	10	2.47	656.76
AA16	1	5	2.91	494.58
AA17	1	6	3.25	508.61
AA18	3	9	-0.97	702.74
AA19	4	9	-1.19	660.71
AA20	3	8	-0.31	644.71
AA21	4	8	-0.54	602.67
AA22	3	6	5.43	501.65
AA23	3	7	5.79	553.77
QAA1	3	7	7.97	539.75
QAA2	3	6	9.42	537.77
QAA3	3	5	9.59	499.68
QAA4	3	10	8.95	607.75
QAA5	3	7	8.78	567.8
QAA6	3	7	8.02	533.72
QAA7	3	7	8.51	533.72
QAA8	3	9	8.55	555.63
QAA9	3	8	7.69	534.71
QAA10	4	6	8.22	493.66
QAA11	3	6	8.5	507.68
QAA12	3	6	8.82	495.65
QAA13	3	5	8.42	463.63
QAA14	3	6	9.11	509.72
QAA15	3	5	8.42	463.63

QAA16	3	4	8.8	446.58
QAA17	3	4	9.24	462.64
QAA18	3	4	9.78	456.61
QAA19	3	5	8.48	457.6
QAA20	3	5	10.12	422.55
QAA21	4	6	8.22	493.66
QAA22	3	6	8.82	495.65
QAA23	3	5	8.42	463.63
QAA24	3	5	8.42	463.63
QAA25	3	5	8.42	463.63
QAA26	3	5	8.53	448.59
QAA27	3	4	9.78	456.61
QAA28	3	5	8.48	457.6
QAA29	3	5	10.12	422.55
QAA30	3	7	8.73	527.66
QAA31	3	7	8.58	525.67
QAA32	3	6	9.49	521.68
QAA33	3	6	9.19	523.7
QAA34	3	8	7.5	543.66
QAA35	3	8	7.35	541.67

The results of rule of five show that all the compounds follow the HBA and HBD constraints but some compounds deviate from the regular rule of five and this is shown in Table 4.2.

As we can see that logP and molecular weight features are not following the Lipinski's rule in many compounds but when compared to the standard drugs, both of the standard drugs have molecular weight greater than 500. Also the logP value is greater than 10. So the result is verified and compatible with the standard drugs concluding that all the potential hits have drug-like properties.

Table 4.2: Detailed Analysis of Rule of Five in percentage form

RULE OF FIVE CONSTRAINT	PERCENTAGE
Hydrogen Bond Acceptor	100%
Hydrogen Bond Donor	100%
Molecular Weight	64%
Log P	74%

4.3 Pharmacophore Modeling

The chemical features of ligands which enhance their binding affinity to the target protein are always of keen importance. The pharmacophore model of anti-cancer drugs has been reported for various microtubule-stabilizing agents (Manetti *et al.*, 2003, Ojima *et al.*, 1999; Giannakakou *et al.*, 2000). But before this, none of the research has taken into account such a large collection of different classes altogether for Pharmacophore model generation. Therefore, this is the first attempt to generate the

general pharmacophore model for a total of seven different microtubule stabilizing classes of compounds.

Technique followed for identifying pharmacophore is that reported by Noureen and collaborators (Noureen *et al.*, 2010). LigandScout was used to generate the pharmacophore model of all the compounds of the data set essentially focusing on the common features such as H-bonding and Hydrophobic volumes. The Figure 4.1 & 4.2 shows the pharmacophore features of standard drugs Docetaxel and Paclitaxel.

Figure 4.3-4.9 represents the 2D and 3D view of the compounds. These compounds are taken as the representative compounds of the different classes i.e. Dictyostatin, Discodermolide, Taccalonolide, Epothilone, Laulimalide, Eleutherobin and Sarcodictyin. In each figure from Figure 4.3-4.9, Ligand Scout suggests that every single compound contains hydrophobic patch (yellow spheres), hydrogen bond donors (Green spheres) and hydrogen bond acceptors (red spheres).

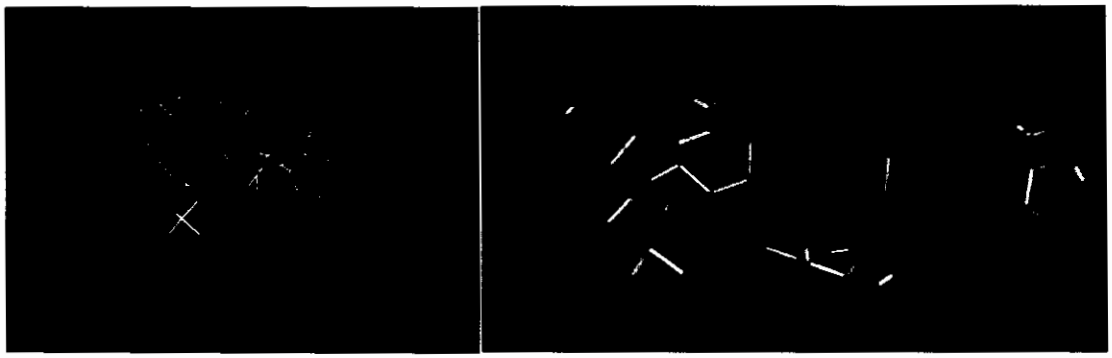

Figure 4.1: Docetaxel: 2D and 3D pharmacophore

Figure 4.2: Paclitaxel: 2D and 3D pharmacophore

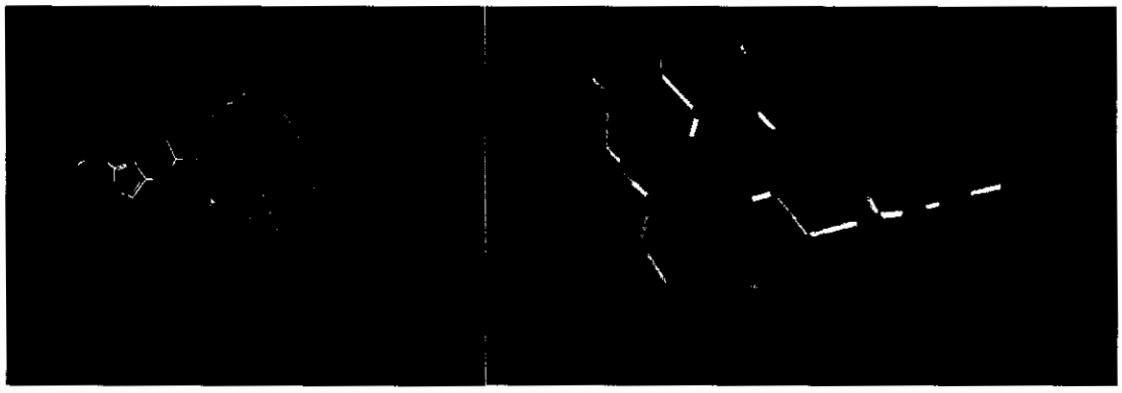

Figure 4.3: Epothilone1: 2D and 3D pharmacophore

Figure 4.4: Dictyostatin: 2D and 3D pharmacophore

Figure 4.5: Discodermolide: 2D and 3D pharmacophore

Figure 4.6: Laulimalide: 2D and 3D pharmacophore

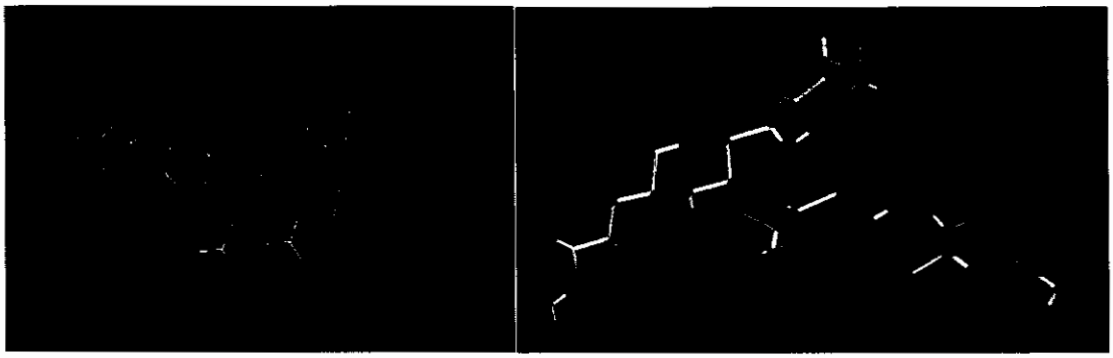

Figure 4.7: Eleutherobin: 2D and 3D pharmacophore

Figure 4.8: Sarcodictyin B: 2D and 3D pharmacophore

Figure 4.9: Taccalonolide: 2D and 3D Pharmacophore

The respective features in each of the compound such as Hydrophobic, HBD, HBA or aromatic are summarized in tabular form in table 4.3.

To generate a pharmacophore model based on several ligands, ligands were superimposed along with standard drugs and the shared pharmacophore was generated as shown in Figure 4.10. The common featured pharmacophore predicted for the seven classes of microtubule stabilizing anti-mitotic agents (MSAAs) against cancer in general and ovarian cancer in particular, is as; three hydrophobic (shown by yellow circles), four Hydrogen Bond Acceptors (shown in red) and one Hydrogen Bond donor (shown in green). The pharmacophoric features help in the identification of better anti-cancer agents.

On the basis of the above information pharmacophore distance triangle was made which is basically three-feature triangle such that it incorporates 1 hydrophobic feature, 1 HBD, and 1 HBA. Distance range is also given for the pharmacophore triangle. These distances were calculated with the help of VMD software. The pharmacophore triangle is given in Figure 4.10b. The distance ranges from minimum to maximum and have been measured between the HBA and HBD, HBA and HP and HBD and HP. The distances between hydrophobic and HBD range from 2.36 Å to 4.39 Å, between hydrophobic to HBA range from 2.22 Å to 4.27 Å and between HBA to HBD range from 2.01Å to 2.86Å.

Table 4.3: Pharmacophore features of the respective compounds

Compounds	HBA	HBD	HP/Aromatic
Epothilone	7	3	10
Dictyostatin	5	4	5
Discodermolide	7	4	10
Laulimalide	6	2	3
Eleutherobin	10	1	4
Sarcodictyin	6	1	4
Taccalonolide	9	3	4

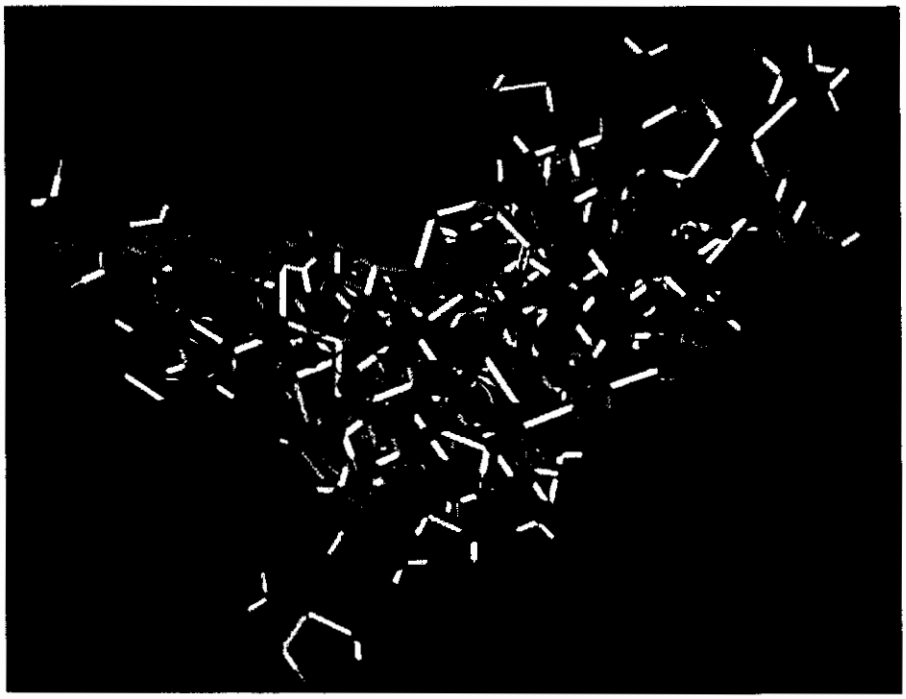

Figure 4.10a: superimposed ligands along with shared features

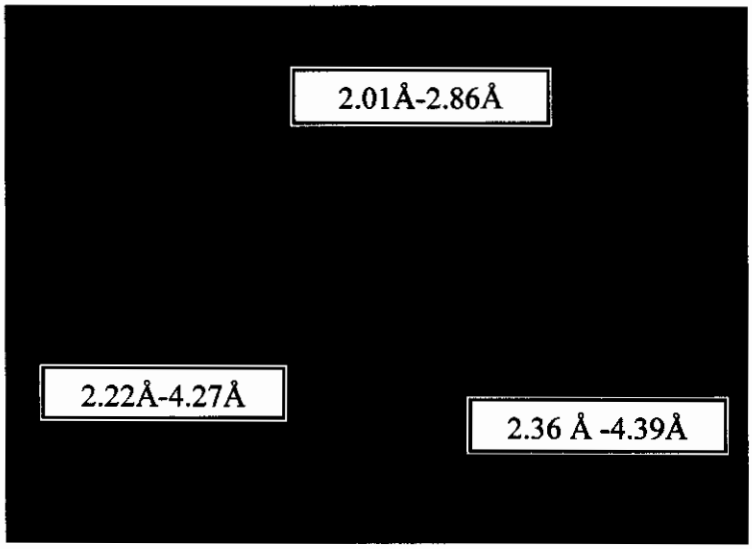

Figure 4.10b: the shared Pharmacophore with the Pharmacophore triangle

Table 4.4: Distance of the compounds incorporated to identify the general pharmacophore model

Compounds	HBA-HBD(Å)	HBD-HP(Å)	HBA-HP(Å)
Epothilones	2.86	2.68	3.39
Dictyostatins	2.34	2.37	2.40
Discodermolides	2.49	2.37	2.36
Laulimalides	2.62	4.39	4.27
Eleutherobins	2.39	3.35	2.33
Sarcodictyins	2.39	3.35	2.33
Taccalonolide	2.01	3.35	2.63
Docetaxel	2.34	2.43	4.21
Paclitaxel	2.19	2.36	2.49

4.4 Molecular field-based similarity analysis

Previously, Cheeseright *et al.* have described molecular fields in a form that enables similarity comparisons across molecules in three dimensions and demonstrated how molecular fields can be used as non-structural templates for defining similar biological behaviour. It has so far shown that field patterns can be used to align molecules that act at the same target by their common field pattern and derive the biologically active conformation of a Ligand without access to any protein structural data (FieldTemplating). The virtual screening of all synthesized compounds was carried out using field patterns for potential hits (Field Aligning). Field Templating and Field Aligning rely on the assumption that those molecules whose field patterns are most similar to those of an active search molecule will be the ones most likely to show the same patterns of biological activity and should be chosen for further investigation.

In the study, two FDA approved standard drugs and one Ligand, Dictyostatin, were used to generate templates with their own field pattern using FieldTemplater. Figure 4.11a shows the template generated through FieldTemplater. Of three highest ranked template sets from FieldTemplater, only top-ranking template set was chosen as the master template set on which to base the calculation of field similarities across the whole data set. The scores for field alignment of the top-rank template set are given in table 4.5. Once a template has been generated, it can be used to align multiple molecules as part of lead optimization process. FieldAlign generates 3D conformers from a 2D molecule and then calculates a field similarity score for each conformer. Figure 4.11b shows the ligands aligned with the template. Figure 4.12 (a-d) is showing the different

fields; hydrophobic, Van Der Waal, positive and negative fields, colored differently in the FieldAlign software. Table 4.6 shows the values for similarity score against each compound when given as input as 2D molecule and aligned with the template through FieldAlign. It identifies, scores, and displays the conformers of the ligands that best match the template. The most probable conformer of each database molecules was selected on the basis of pair wise matching and close observation of molecular field point alignment.

Figure 4.11a & b: (a) field alignment of template molecules in lowest energy conformations **(b)** field alignment of all MSAAs to the template ((the positive (red), negative (Blue), Van der Waals (yellow), and hydrophobic (orange) field point are represented as balls or cubes or polygons)

Figure 4.12a & b: Hydrophobic field points (Gold) & van der Waals surface field points (yellow)

Figure 4.12c & d: Negative field points likely to interact with HBD (blue) & positive field points likely to interact with HBA (red)

Table 4.5: Scores for Top-Rank Template

S. No.	Template score	Value of score
1	Molecular similarity	0.482
2	Field similarity	0.422
3	Shape similarity	0.542

Table 4.6: Similarity scores after alignment of MSAAs with template

Compound	Similarity score
Epothilone	0.493
Eleutherobin	0.444
Laulimalide	0.48
Taccalonolide	0.416
Sarcodictyin	0.434
Discodermolide	0.452

4.5 Molecular Docking

Docking studies have been performed for the seven classes of compounds as well as standard drugs using ADTools and Autodock Vina.

4.5.1 Active Site of Tubulin

Tubulin protein has three binding sites viz.; Vinca Alkaloid site, Colchicine-binding site and Tubulin-binding site. The data set was docked and found to bind at the same active site position i.e., Tubulin-binding site; the active site amino acids were identified by looking the 5 Å vicinity. Table 4.7 show the list of all the amino acid within 5 Å of the ligand docked with Tubulin. The residues that are significant for binding interactions and thus comprising the binding pocket are: PHE272, VAL23, GLU27, ALA233, PRO360, PRO274, HIS229, ARG278, LEU371, GLY370, GLN282, ARG369, THR276, LEU230, LEU275, ASP226, GLY225, ASP26, LEU217, LEU219, SER236, PHE83, SER277, ARG284, LEU286 and LYS218. The study revealed that PHE272, VAL23, GLU27, ALA233, PRO360, HIS229, ARG278, GLY370, THR276, LEU275, ASP26, LEU217 and ARG284 are almost always included in the active site amino acid residues. The results coordinate well with the already shown experimental data.

Table 4.7: Active site amino acid residues

A.A.	AA1	AA2	AA3	AA4	AA5	AA6	AA7	AA8	AA9	AA10	AA11	AA12
PHE272	Y	Y	Y	Y	N	Y	Y	Y	Y	Y	Y	N
VAL23	Y	Y	Y	Y	N	Y	Y	Y	N	N	N	Y
GLU27	Y	Y	Y	N	N	Y	N	N	N	N	N	N
ALA233	Y	Y	Y	Y	N	N	N	N	Y	Y	Y	Y
PRO360	Y	Y	Y	Y	N	Y	Y	Y	N	N	Y	Y
PRO274	Y	N	Y	Y	Y	Y	N	N	N	N	N	N
HIS229	Y	N	Y	Y	Y	Y	Y	Y	Y	Y	Y	Y
ARG278	Y	Y	Y	Y	N	Y	N	N	Y	N	Y	Y
LEU371	Y	Y	Y	Y	Y	Y	N	Y	Y	N	N	Y
GLY370	Y	N	N	Y	Y	Y	N	N	N	N	N	Y
GLN282	Y	Y	N	N	N	N	N	N	Y	N	Y	Y
ARG369	Y	Y	Y	Y	Y	N	N	N	N	N	N	N
THR276	N	N	N	Y	Y	Y	N	N	N	N	N	N
LEU230	N	N	N	Y	N	N	N	Y	Y	Y	N	Y
LEU275	N	N	N	Y	Y	N	Y	Y	Y	Y	Y	Y
ASP226	N	N	N	Y	N	N	N	Y	N	N	N	N
GLY225	N	N	N	Y	Y	N	N	N	N	N	N	N
ASP26	N	N	N	Y	Y	Y	Y	N	N	N	N	N
LEU217	N	N	N	Y	Y	Y	Y	Y	N	Y	Y	Y
LEU219	N	N	N	Y	N	N	N	N	N	N	N	N
SER236	N	N	N	N	N	Y	N	N	N	N	N	N
PHE83	N	N	N	N	N	N	Y	N	N	N	N	N
SER277	N	N	N	N	N	N	N	Y	N	Y	Y	N
ARG284	N	N	N	N	N	N	N	N	Y	N	N	N
LEU286	N	N	N	N	N	N	N	N	Y	N	N	N
LYS218	N	N	N	N	N	N	N	N	N	Y	N	N

A.A.	AA14	AA15	AA16	AA17	AA18	AA19	AA20	AA21	AA22	QAA2	QAA3
PHE272	N	Y	Y	Y	Y	Y	Y	Y	Y	Y	N
VAL23	N	N	N	N	N	N	N	N	Y	N	N
GLU27	N	N	N	N	N	N	N	N	N	N	N
ALA233	N	N	Y	Y	Y	Y	N	N	Y	N	N
PRO360	N	Y	Y	Y	N	Y	N	N	Y	Y	N
PRO274	Y	Y	N	N	N	Y	N	Y	N	N	N
HIS229	N	Y	Y	Y	Y	Y	Y	Y	N	Y	Y
ARG278	Y	Y	N	Y	Y	Y	N	Y	Y	Y	N
LEU371	Y	Y	Y	Y	Y	Y	Y	Y	Y	N	Y
GLY370	Y	N	Y	Y	Y	Y	Y	Y	Y	Y	Y
GLN282	Y	N	N	Y	N	Y	Y	Y	Y	Y	Y
ARG369	N	Y	N	N	N	Y	N	Y	N	Y	N
THR276	Y	Y	N	Y	N	N	N	N	Y	Y	Y
LEU230	N	N	N	N	N	N	N	N	N	N	Y
LEU275	N	N	Y	Y	Y	N	Y	N	N	N	N
ASP226	N	N	Y	N	N	N	N	N	N	N	Y
GLY225	N	N	N	N	N	N	N	N	N	N	N
ASP26	N	Y	N	N	N	N	N	N	N	N	N
LEU217	Y	N	Y	N	Y	N	N	N	N	N	Y
LEU219	N	N	N	N	N	N	N	N	N	N	N
SER236	N	N	N	N	N	N	N	N	Y	N	N
PHE83	N	N	N	N	N	N	N	N	N	N	N
SER277	N	Y	N	Y	N	N	N	N	Y	N	N
ARG284	Y	Y	N	N	N	Y	N	Y	Y	N	N
LEU286	N	N	N	N	N	N	N	N	N	N	N
LYS218	N	N	N	N	N	N	N	N	N	N	N

4.5.2 Molecular Docking Of Standard Drugs

A detailed 3D analysis of the docked site of these compounds indicated that they bind to same active site. Table 4.8 enlists all the three types of interactions of the standard drugs Docetaxel and Paclitaxel. The interactions are built manually with the aid of VMD software by selecting each time an atom from the ligand and an atom from the protein. The software then automatically gives the distance between the two. If the distance is within 4 Å, the interaction was kept else it was removed. The interactions include Hydrogen, Ionic and Hydrophobic. Hydrogen bond is formed when Hydrogen binds with either Oxygen or Nitrogen. When Oxygen forms a bond with Nitrogen, it gives ionic bonding. Hydrophobic interaction is formed when Carbon binds with Carbon. While Figure 4.13 & 4.14 shows these interactions. The interactions will be then compared with the selected lead compound.

Docking of Docetaxel with the protein 1JFF gave number of interactions that includes 1 ionic, 3 Hydrogen and 18 hydrophobic. Oxygen of Docetaxel form bond with Nitrogen of ARG278 at a distance of 3.51.

Hydrogen forms interactions with Oxygens of THR276 at 3.15 and 3.14 and with Oxygen of GLY370 at a distance of 2.98.

The hydrophobic interactions include Carbons of PRO274 at the distance 3.76; LEU371 at 3.81, 3.79 and 3.87; LEU217 at 3.87; GLN282 at 3.88, 3.69,

3.61 and 3.67; PHE272 at 3.96 and 3.66; Arg278 at 3.91, 3.89, 3.87, 3.38, 3.35, 3.68 and 3.75 making bonds with Carbons of Docetaxel.

The binding interactions of Paclitaxel include 2 ionic and Hydrogen bondings each and 27 hydrophobic interactions.

Oxygen of Paclitaxel binds with Nitrogen of ARG278 and HIS229 at distances 3.57 and 2.97 respectively. Hydrogens bind with Nitrogen of HIS229 in two different conformations at the distances of 3.25 and 3.90. The hydrophobic interactions include Carbons of PHE272 at 3.535, 3.76, 3.54 and 3.63; ALA233 at 3.442, 3.63, 3.58, 3.993; VAL23 at 3.134, 3.86, 3.73 and 3.88; GLU22 at 3.82; HIS229 at 3.97 and 3.80; ASP26 at 3.46, 3.85, 3.78 and 3.59; GLN282 at 3.47 and 3.48; ARG278 at 3.78; LEU217 at 3.76; LEU371 at 3.81, 3.53, 3.31and PRO274 at 3.98 interacting with Carbons of Paclitaxel.

Table 4.8: Hydrogen, Ionic and hydrophobic interactions of the standard drugs

Name	Ionic		Hydrogen		Hydrophobic		IC50
	Bond	Distance	Bond	Distance	Bond	Distance	
DOCE	ARG278:N	3.51	THR276:O	3.15	PRO274:CB	3.76	0.0004
			THR276:O	3.14	LEU371:CD1	3.81	
			GLY370:O	2.98	LEU371:CD2	3.79	
					LEU371:CD1	3.87	
					LEU217:CD2	3.87	
					GLN282:CB	3.88	
					GLN:282:CG	3.69	
					GLN282:CG	3.61	
					GLN282:CD	3.67	
					PHE272:CZ	3.96	
					PHE272:CE2	3.66	
					ARG278:CZ	3.91	
					ARG278:CZ	3.89	
					ARG278:CG	3.87	
					ARG278:CG	3.38	
					ARG278:CG	3.35	
					ARG278:CG	3.68	
					ARG278:CG	3.75	
PTX	ARG278:NE	3.57	HIS229:NE2	3.25	PHE272:CZ	3.535	0.001
	HIS229:NE2	2.97	HIS229:NE2	3.90	ALA233:CB	3.442	
					ALA233:CA	3.993	
					VAL23:CG1	3.134	
					VAL23:CG1	3.86	
					VAL23:CG1	3.73	
					VAL23:CG1	3.88	
					GLU22:C	3.820	
					HIS229:CD2	3.971	
					ASP26:CG	3.457	
					ASP26:CB	3.592	
					GLN282:CB	3.478	
					ARG278:CZ	3.780	
					LEU217:CD2	3.755	
					GLN282:CB	3.484	
					LEU371:CD1	3.808	
					LEU371:CD2	3.527	
					PHE272:CZ	3.756	
					ALA233:CA	3.627	
					ALA233:CB	3.583	
					HIS229:CD2	3.801	
					ASP26:CG	3.847	
					ASP26:CB	3.782	
					PRO274:CB	3.975	
					PHE272:CE1	3.625	
					LEU371:CD1	3.306	
					PHE272:CZ	3.54	

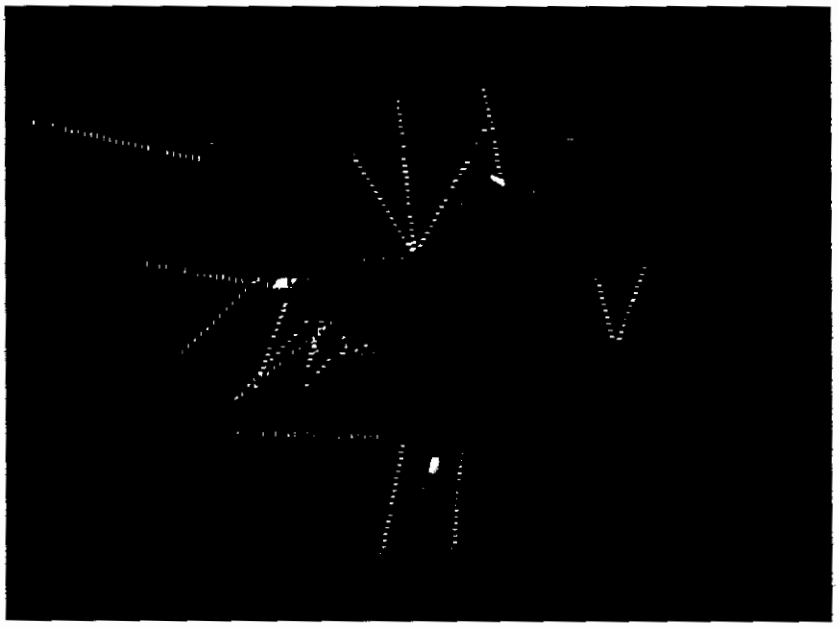

Figure 4.13: Amino acid residues of active site of 1JFF bind with Docetaxel

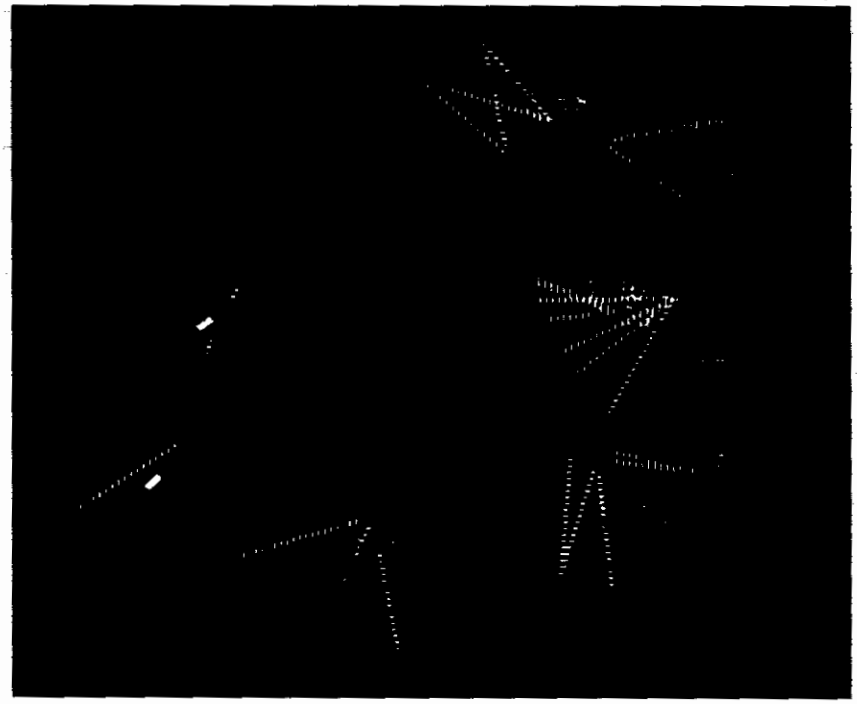

Figure 4.14: Amino acid residues of active site of 1JFF bind with Paclitaxel

4.5.3 Molecular Docking Of Selected Ligands

Various conformations were obtained for the ligands docked into the target Tubulin protein with PDB ID 1JFF. Amongst them, one was selected on the basis of binding affinity value which is usually taken in Kcal/mol. The ranking is auomatically assigned to these conformations by the docking program. Starting from the minimum binding affinity value, it ranks till the last conformation. So, the most active conformation is the one with the least energy affinity value. Along with it, the IC50 values are also taken into consideration. Figures 4.15a and 4.15b show the docked conformations of the two compounds as examples. The images are obtained using LigandScout. The ligands are shown in sticks form while the environment is shown in line style. The protein backbone is in ribbon form. The active conformations of the ligands were used for the prediction of their interactions. Binding affinity values along with the names of compounds are given in the table 4.9.

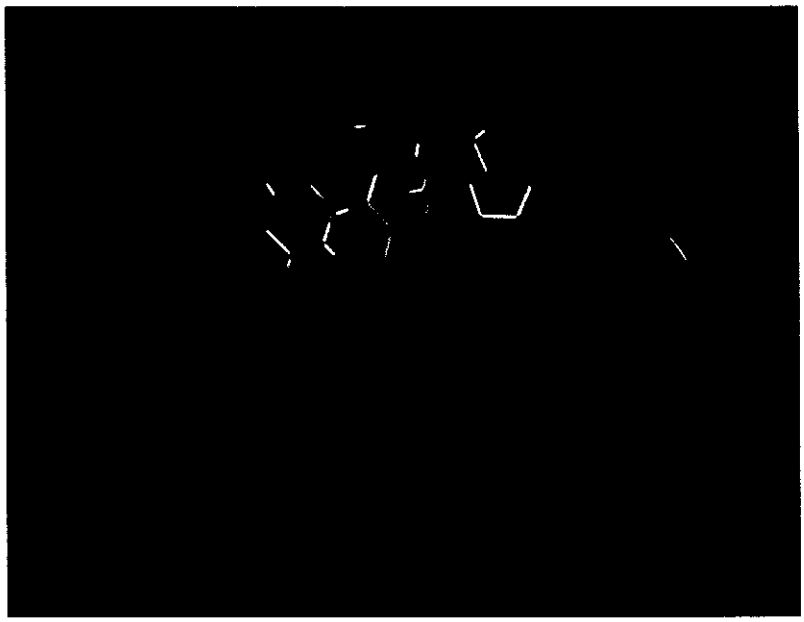

Figure 4.15a: Active conformation of Taccalonolide B (AA20)

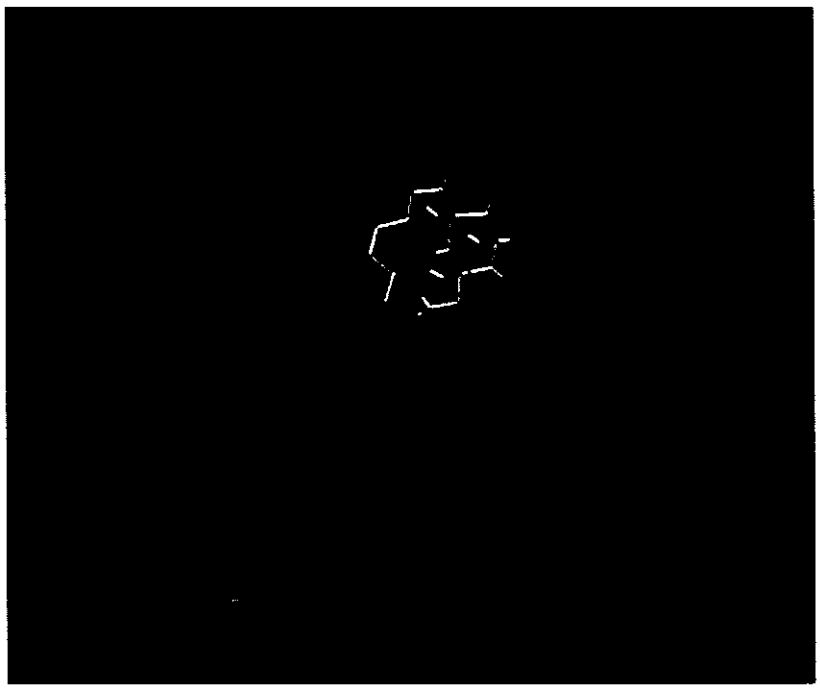

Figure 4.15b: Active conformation of Epothilone (AA20)

Table 4.9: The docking Data Set and their Energy Affinity Values

Compound No.	Names[1]	Energy value (Kcal/mol)
AA1	Dictyostatin	-11.7
AA2	16-desmethyl Dictyostatin	-10.0
AA3	9-methoxy Dictyostatin	-11.9
AA4	Discodermolide	-10.5
AA5	Discodermolide1	-10.1
AA6	Discodermolide2	-7.0
AA7	Discodermolide3	-9.9
AA8	Discodermolide4	-7.1
QAA1	Epothilone1	-9.5
QAA2	Epothilone2	-7.9
AA22	Epothilone3	-9.4
QAA3	Epothilone4	-8.5
AA23	Epothilone5	-9.1
AA9	Laulimalide	-8.5
AA10	16-desmethyl laulimalide	-9.0
AA11	Eleutherobin	-10.2
AA12	Eleuthoside A	-10.4
AA13	Eleuthoside B	-8.7
AA14	DesacetylEleuthrobin	-10.1
AA15	isoEleuthrobin A	-8.8
AA16	Sarcodictyin A	-10.4
AA17	Sarcodictyin B	-7.9
AA18	TaccalonolideA	-11.9
AA19	TaccalonolideB	-7.5
AA20	TaccalonolideE	-10.9
AA21	TaccalonolideN	-7.6
DOCE	Docetaxel	-12.2
PTX	Paclitaxel	-12.4

[1] As given in literature

4.5.3.1 Interactions of Ligands with the Target Protein

As discussed before, the interactions between the ligands and protein have been predicted using VMD. It proved to be a tedious task studying interactions for 24 compounds and two standards. The three kinds of binding interactions including Hydrogen Bonding, Hydrophobic and ionic Interactions and their distances for the complete data Set along with IC50 values are shown in the table 4.10.

Table 4.10: Binding Interactions and distances of Data Set showing all the three kinds of interactions including Hydrogen Bonding, Hydrophobic and ionic Interactions

S.No.	Ionic		Hydrogen		Hydrophobic		IC50
	Bond	Distance	Bond	Distance	Bond	Distance	
AA1			PRO274:O	2.29	PHE272:CZ	3.795	0.0098
					PHE272:CE1	3.796	
					PHE272:CZ	3.801	
					PHE272:CZ	3.56	
					PHE272:CE2	3.906	
					PHE272:CE2	3.93	
					VAL23:CG1	2.792	
					VAL23:CG1	3.307	
					VAL23:CG1	3.766	
					GLU27:CG	3.910	
					GLU27:CB	3.584	
					GLU27:CD	3.655	
					GLU27:CG	3.91	
					ALA233:CA	3.800	
					ALA233:CA	3.78	
					ALA233:CB	3.570	
					ALA233:CB	3.51	
					PRO360:C	3.776	
					PRO360:CA	3.82	
					PRO360:CB	3.980	
					PRO360:CB	3.21	
					HIS229:CE1	3.827	
					ARG278:CA	3.385	
					ARG278:C	3.72	
					LEU371:CD1	3.76	
					LEU371:CD1	3.67	
					LEU371:CD1	3.65	
					LEU371:CD2	3.98	
					LEU371:CD2	3.83	
					GLY370:C	3.55	
AA2					ALA233:CA	3.74	
			GLU27:OE2	3.49	ALA233:CA	3.70	1.5
					ALA233:CB	3.31	
					PRO360:C	3.79	
					PRO360:CB	3.21	
					PRO360:CA	3.87	
					PRO360:CA	3.95	
					PRO360: C	3.93	
					PRO360:CB	3.45	
					PRO360:CB	3.73	
					VAL23:CG1	3.46	
					VAL23:CG1	3.97	
					PHE272:CZ	3.87	
					PHE272:CE1	3.717	
					PHE272:CZ	3.89	
					LEU371:CB	3.88	

					ASP226:CG	3.849	
					ASP226:CB	3.305	
					ASP226:CA	3.795	
					HIS229:CD2	3.691	
					LEU219:CD1	3.743	
					LEU219:CD2	3.572	
					LEU217:CD2	3.653	
					ARG278:CG	3.845	
					ARG278:CB	3.698	
AA5	GLY370:N	3.671	PRO274:O	3.009	ASP26:CG	3.924	0.0061
	THR276:N	3.318	THR276:O	3.011	ARG369:CB	3.712	
	HIS229:NE2	3.948	THR276:N	3.086	ARG369:CB	3.947	
	HIS229:NE2	3.925	THR276:OG	3.839	ARG369:CB	3.813	
			HIS229:NE2	3.809	GLY370:CA	3.632	
			HIS229:NE2	3.069	GLY370:CA	3.722	
					GLY370:C	3.984	
					LEU371:CB	3.930	
					LEU371:CD1	3.647	
					LEU371:CD2	3.489	
					LEU275:CD1	3.521	
					LEU217:CD2	3.809	
					LEU217:CD2	3.590	
					LEU217:CG	3.609	
					LEU217:CD2	3.828	
					LEU217:CG	3.797	
					LEU217:CD2	3.909	
					HIS229:CD2	3.797	
					GLY225:CA	3.862	
					GLY225:C	3.679	
AA6	PRO360:O	3.127	GLY370:N	2.596	SER236:CB	3.884	0.022
	GLY370:N	3.240	GLY370:O	3.833	PRO360:CB	3.822	
	LEU275:N	3.791	LEU371:N	2.307	GLU27:CD	3.789	
	THR276:N	2.800	PRO360:O	2.266	VAL23:CG1	3.696	
			ARG369:N	3.866	GLU27:CB	3.787	
			LEU371:N	3.561	GLU27:CD	3.772	
			PRO360:O	3.918	GLU27:CG	3.748	
			PRO274:O	3.805	PRO360:CA	3.781	
			THR276:OG	2.169	PRO360:CB	3.750	
			THR276:O	2.736	VAL23:CG1	3.717	
			THR276:N	2.759	ASP26:CG	3.861	
					VAL23:CG1	3.640	
					HIS229:CE1	3.754	
					VAL23:CG1	3.808	
					PRO360:CB	3.911	
					PRO360:C	3.832	
					PHE272:CE2	3.828	
					PHE272:CZ	3.887	
					PHE272:CE2	3.836	
					LEU217:CD2	3.611	
					LEU217:CG	3.878	
					LEU371:CD1	3.846	
					LEU371:CD1	3.750	
					LEU371:CD1	3.630	

					LEU371:CG	3.82	
					LEU371:CD2	2.92	
					LEU371:CD1	3.71	
					LEU371:CD1	3.68	
					GLN282:CB	3.77	
					ARG278:CA	3.61	
					ARG278:CA	3.43	
					ARG369:CB	3.82	
					PHE272:CE1	3.813	
AA3			PRO274:O	2.37	PHE272:CE2	3.955	0.0082
					PHE272:CZ	3.833	
					PHE272:CZ	3.821	
					PHE272:CE2	3.947	
					VAL23:CG1	2.810	
					VAL23:CG1	3.305	
					VAL23:CG1	3.750	
					GLU27:CG	3.887	
					GLU27:CD	3.616	
					ALA233:CB	3.989	
					ALA233:CA	3.751	
					ALA233:CB	3.479	
					PRO360:CB	3.930	
					PRO360:CB	3.962	
					PRO360:CA	3.837	
					PRO360:C	3.702	
					ARG278:C	3.731	
					ARG369:CB	3.982	
					LEU371:CD1	3.692	
					LEU371:CD1	3.644	
					HIS229:CE1	3.803	
	ARG369:N	3.748	PRO274:O	2.328	ASP26:CG	3.879	
AA4	GLY370:N	2.811	LEU275:N	3.593	VAL23:CG1	3.650	0.0065
	THR276:N	3.008	THR276:OG	3.959	VAL23:CG1	3.689	
	LEU230:N	3.313	THR276:N	3.193	ALA233:CA	3.876	
	HIS229:ND1	3.034	THR276:O	3.732	ALA233:CB	3.728	
	HIS229:NE2	3.882	LEU230:N	3.312	PRO360:CB	3.696	
	LEU275:N	3.99	HIS229:ND1	3.223	PHE272:CE2	3.426	
			ASP226:O	3.077	PHE272:CZ	3.958	
			ASP226:N	3.756	PHE272:CE2	3.763	
			ASP226:OD2	2.823	LEU371:CD1	3.688	
			GLY225:O	3.210	LEU371:CD2	3.597	
			ASP226:N	3.302	PRO274:CB	3.953	
			ASP226:O	3.834	HIS229:CE1	3.815	
			ASP226:OD2	3.465	HIS229:CE1	3.379	
					HIS229:CE1	3.982	
					LEU217:CD2	3.698	
					LEU230:CB	3.871	
					LEU217:CD2	3.705	
					LEU217:CG	3.561	
					LEU217:CD1	3.832	
					HIS229:CG	3.822	
					LEU219:CD2	3.575	
					LEU217:CD2	3.878	

					ARG278:CG	3.703	
					ARG278:CA	3.789	
	ASP26:OD2	2.986	ASP26:OD2	2.866	PHE83:CZ	3.795	
AA7			ASP26:OD2	3.242	ASP26:CB	3.721	0.0065
					ASP26:CB	3.700	
					VAL23:CA	3.801	
					VAL23:CG1	3.846	
					VAL23:CG1	3.378	
					HIS229:CE1	3.984	
					PRO360:CB	3.874	
					PHE272:CZ	3.787	
					PHE272:CE2	3.984	
					PHE272:CE2	3.642	
					HIS229:CE1	3.725	
					HIS229:CE1	3.938	
					LEU275:CD1	3.772	
					LEU217:CD2	3.483	
					HIS229:CE1	3.975	
					LEU217:CD2	3.305	
					HIS229:CD2	3.610	
					HIS229:CE1	3.926	
	ASP226:O	3.35	ASP226:O	3.11	PRO360:CB	3.551	
AA8	HIS229:ND1	3.18	ASP226:O	2.88	PRO360:CB	3.896	0.035
	HIS229:NE2	3.54	HIS229:ND1	3.24	PRO360:CA	3.657	
			HIS229:ND1	3.68	VAL23:CG1	3.335	
			LEU230:N	2.64	VAL23:CG1	3.747	
					VAL23:CG1	3.934	
					PHE272:CZ	3.878	
					LEU275:CD1	3.505	
					LEU275:CD1	3.274	
					LEU275:CD1	3.830	
					PHE272:CE2	3.734	
					PHE272:CD2	3.799	
					PHE272:CD2	3.874	
					PHE272:CE2	3.923	
					LEU371:CD2	3.848	
					LEU371:CD1	3.75	
					HIS229:CE1	3.711	
					HIS229:CE1	3.512	
					HIS229:CE1	3.865	
					LEU217:CD2	3.432	
					LEU217:CG	3.800	
					SER277:C	3.702	
					SER277:CA	3.674	
	HIS229:NE2	3.62	ARG278:O	3.75	PHE272:CZ	3.76	
AA9	HIS229:ND1	3.43			PHE272:CE2	3.44	0.026
	ARG278: N	3.76			PHE272:CE2	3.65	
					PHE272:CD2	3.55	
					LEU275:CD1	3.58	
					LEU230:CA	3.67	
					LEU217:CD2	3.50	
					LEU217:CD2	3.76	
					LEU217:CD2	3.67	

					LEU217:CD2	3.71	
					LEU217:CD	3.89	
					HIS229:CE1	3.84	
					HIS229:CE1	3.91	
					HIS229:CE1	2.94	
					LEU371:CD1	3.99	
					LEU230:CA	3.94	
					ARG284:CD	3.71	
					ARG284:CA	3.72	
					ARG284:CA	3.86	
					GLN282:CA	3.97	
					LEU286:CD1	3.61	
					LEU286:CD1	3.80	
					LEU371:CD1	3.70	
					LEU371:CD1	3.79	
					ALA233:CD	3.64	
					LEU230:CB	3.97	
AA10					LEU230:CA	3.66	0.028
					ALA233:CB	3.70	
					PHE272:CE2	3.81	
					HIS229:CE1	3.85	
					LEU275:CD1	3.79	
					LEU275:CD1	3.59	
					LEU217:CG	3.88	
					LEU217:CG	3.40	
					LEU217:CB	3.44	
					LEU217:CA	3.91	
					LEU217:CD2	3.78	
					SER277:CA	3.76	
					SER277:CA	3.74	
					LEU219:CD2	3.91	
					LEU219:CD1	3.93	
					SER277: CB	3.82	
					LYS218: CB	3.79	
	ARG278:NE	3.55	ARG278:NE	2.33	GLN282:CD	3.63	
AA11	ARG278:NE	2.86	ARG278:NH2	2.81	ARG278:CG	3.97	0.04
	ARG278:NH2	3.59			ARG278:CB	3.52	
					ARG278:CB	3.94	
					SER277:CA	3.88	
					LEU217:CD2	3.78	
					LEU217:CG	3.53	
					PRO360:CB	3.95	
					ALA233:CB	3.51	
					PRO360:CB	3.19	
					PHE272:CZ	3.93	
					LEU275:CD1	3.91	
					PHE272:CE2	3.96	
					ALA233:CA	3.79	
					HIS229:CE1	3.86	
	GLY370:N	3.64			LEU230:CD1	3.92	
AA12	HIS229:NE2	3.53			LEU217:CD2	3.67	0.034
	HIS229:ND1	3.59			LEU275:CD1	3.67	
					LEU230:CB	3.48	

					LEU230:CA	3.91	
					HIS229:CE	3.93	
					GLN282:CG	3.86	
					ARG278:CG	3.60	
					VAL23:CG1	3.58	
					PRO360:CB	3.91	
					PRO360:CB	3.48	
					PRO360:CB	3.54	
					PRO360:CB	3.99	
					LEU371:CD1	3.75	
					LEU371:CD2	3.91	
					LEU371:CD1	3.68	
					LEU371:CD2	3.60	
					PRO360:C	3.79	
					LEU275:CD1	3.53	
					ALA233:CA	3.75	
AA13	ARG390:NH2 LYS176:N	3.57 3.79	ALA304:O	3.80	LYS229:CA LYS299:CA ARG390:CD PRO175:CB PRO175:CG ASP211:CG ILE212:CD1 ILE212:CG1 GLU386:CD ALA304:C	3.82 3.84 3.98 3.31 3.66 3.98 3.39 3.42 3.94 3.99	0.022
AA14	ARG284:NH1	2.90	THR276:O	3.91	GLY370:CA LEU371:CD1 LEU371:CD1 LEU371:CD1 ARG278:CA GLN282:CG LEU371:CB PRO274:CB PRO274:C GLY370:C ARG278:CG ARG278:CB LEU217:CD2	3.90 3.79 3.48 3.30 3.38 3.55 3.69 3.26 3.72 3.59 3.40 3.90 3.69	0.04
AA15	ASP26:OD2 ASP26:OD1 ASP26:OD2 ARG284:NH1	3.37 3.73 3.72 3.12	THR276:OG1 ARG278:O SER277:O	2.91 2.78 2.88	PHE272:CE2 PHE272:CD2 LEU371:CB LEU371:CG LEU371:CD2 PRO360:CB PRO274:CB ARG284:CA ARG284:CD HIS229:CE1 LEU371:CD1 ARG369:CB ARG369:CB ASP26:CG	3.81 3.70 3.64 3.86 3.32 3.96 3.95 3.78 3.46 3.64 3.81 3.84 3.84 3.92	0.05

					ASP26:CG	3.98	
AA16	HIS229:NE2	3.81	GLY370:N	3.35	PHE272:CD2	3.86	0.32
	HIS229:ND1	3.83			PHE272:CE2	3.75	
	GLY370:N	3.27			LEU371:CD2	3.04	
	LEU371:N	3.79			LEU371:CD1	3.88	
	LEU371:N	3.81			LEU371:CG	3.70	
					PHE272:CE2	3.81	
					LEU275:CD1	3.95	
					PHE272:CE2	3.56	
					ALA233:CB	3.75	
					LEU217:CD2	3.96	
					ASP226:CA	3.88	
					PRO360:CB	3.41	
					LEU230:CB	3.69	
					HIS229:CE1	3.51	
					LEU371:CB	3.64	
					LEU371:CB	3.68	
					ASP226:C	3.83	
					LEU371:CD2	3.89	
					HIS229:CE1	3.63	
					HIS229:CE1	3.66	
					ALA233:CB	3.97	
AA17	THR276:OG1	3.41	PRO360:O	3.74	PHE272:CE2	3.69	0.3
	THR276:OG1	3.97	GLY370:N	3.28	PHE272:CD2	3.76	
	THR276:O	3.78	LEU371:N	3.59	PHE272:CE2	3.62	
	SER277:O	3.68			PHE272:CE2	3.76	
	LEU371:N	3.40			HIS229:CE1	3.60	
	GLY370:N	3.79			LEU371:CD2	3.78	
	ARG278:O	3.48			LEU371:CG	3.79	
					PRO360:CG	3.88	
					PRO360:CB	3.81	
					PRO360:CB	3.55	
					PRO360:C	3.85	
					PHE272:CZ	3.86	
					GLN282:CA	3.96	
					LEU275:CD1	3.91	
					LEU371:CD1	3.93	
					ALA233:CB	3.66	
AA18	HIS229:NE2	3.97	GLY370:O	3.09	PHE272:CE2	3.67	0.622
	HIS229:ND1	2.95			PHE272:CE2	3.95	
	ARG278:N	3.29			PHE272:CD2	3.92	
	LEU371:N	3.97			GLY370:C	3.86	
					LEU217:CD2	3.70	
					ARG278:CA	3.86	
					LEU371:CD1	3.43	
					LEU275:CD1	3.85	
					LEU275:CD1	3.82	
					LEU275:CD1	3.22	
					LEU371:CB	3.88	
					HIS229:CD2	3.88	
					HIS229:CE1	3.67	
					HIS229:CE1	3.76	
					ALA233:CB	3.78	

AA19	ARG284:NH1	3.04	PRO274:O	3.42	PRO360:CB PRO360:C ALA233:CB HIS229:CE1 PHE272:CE2 ARG278:CG GLN282:CG GLY370:C HIS229:CE1 GLY370:CA LEU371:CD2 ARG278:CG GLN282:CB LEU371:CD1 ARG369:CB	3.89 3.69 3.75 3.53 3.63 3.70 3.82 3.85 3.67 3.77 3.78 3.97 3.74 3.54 3.60	0.208
AA20	HIS229:ND1 HIS229:NE2 LEU371:N	3.00 3.97 3.97	GLY370:O	3.07	LEU275:CD1 PHE272:CE2 PHE272:CD2 HIS229:CE1 HIS229:CE1 LEU371:CD1 PHE272:CE2 GLN282:CB LEU275:CD1 LEU371:CB LEU371:CB LEU275:CD1	3.80 3.70 3.95 3.81 3.88 3.39 3.99 3.87 3.81 3.87 3.77 3.25	0.708
AA21	ARG284:NH1	3.07	PRO274:O	2.50	ARG369:CB HIS229:CE1 HIS229:CE1 HIS229:CE1 PHE272:CE2 GLY370:C GLY370:CA ARG278:CG ARG278:CG LEU371:CD2 GLN282:CB LEU371:CD1	3.54 3.68 3.75 3.55 3.60 3.87 3.74 3.63 3.92 3.76 3.72 3.58	0.201
QAA1	GLN293:N ASN339:ND2 ASN339:ND2 LYS338:NZ GLN293:N	3.850 3.062 3.227 3.548 3.960	GLN293:N THR292:O ASN339:ND2 ASN339:OD1	3.17 2.00 3.86 3.30	PRO289:CB PRO289:C PRO289:CG PRO289:CB PRO289:CB GLN293:CB GLN293:CB GLN293:CA GLN293:CA GLU290:CG PRO289:CB PRO289:CB	3.683 3.984 3.956 3.634 3.889 3.727 3.81 3.19 3.92 3.685 3.866 3.507	0.0002
QAA2	ARG278:N	3.672	ARG278:N THR276:O	3.713 3.626	ARG369:CB PHE272:CE1	3.698 3.989	0.0001

					PHE272:CZ	3.538	
					HIS229:CE1	3.655	
					PRO360:CB	3.963	
					GLY370:CA	3.382	
					GLY370:CA	3.779	
					GLY370:CA	3.958	
					GLY370:C	3.867	
					GLY370:C	3.894	
					GLY370:C	3.954	
					GLN282:CB	3.593	
					ARG278:CG	3.458	
					ARG278:CG	3.804	
					ARG278:CA	3.957	
					ARG278:C	3.708	
	GLY370:N	3.776	ARG284:NH	3.753	ARG278:CG	3.376	
AA22	LEU371:N	3.282	THR276:O	1.930	ARG278:C	3.820	0.0003
	ARG278:N	3.615	THR276:OG	3.608	GLN282:CG	3.858	
	GLN282:N	3.976	ARG278:N	3.769	SER236:CB	3.530	
			SER277:O	3.660	VAL23:CG1	3.230	
					ALA233:CA	3.591	
					ALA233:CB	3.885	
					ALA233:CA	3.855	
					PRO360:CB	3.687	
					PHE272:CZ	3.779	
					VAL23:CG1	3.603	
					ALA233:CA	3.983	
					PHE272:CZ	3.621	
					PHE272:CE2	3.752	
					PHE272:CZ	3.826	
					LEU371:CD2	3.321	
					ARG278:CG	3.771	
					GLN282:CB	3.789	
	THR276:N	3.94	THR276:OG1	3.29	ASP226:CA	3.955	
QAA3			GLY370:O	3.22	HIS229:CG	3.838	0.0035
					LEU230:CA	3.875	
					HIS229:CB	3.885	
					LEU230:CB	3.683	
					ASP226:C	3.781	
					HIS229:CE1	3.671	
					HIS229:CE1	3.859	
					LEU217:CD2	3.743	
					LEU217:CG	3.959	
					LEU275:CD1	3.913	
					LEU217:CD2	3.605	
					LEU217:CD2	3.836	
					LEU230:CB	3.93	
					GLN282:CG	3.540	
					GLN282:CG	3.972	
					LEU371:CD1	3.885	
					GLN282:CB	3.680	
	ARG253:NH1	2.98	PRO162:O	3.84	ASP199:CG	3.768	
AA23	ARG253:NH1	3.05	ARG253:NH1	3.24	ASP199:CG	3.489	0.0035
	VAL257:O	3.94			PRO263:CA	3.503	

	VAL260:O	3.24			VAL257:CA ILE165:CG2 PRO263:CB VAL257:CG1 VAL257:CG1 VAL257:CG1 ASP199:CB VAL257:CG2	3.968 3.573 3.983 3.835 3.869 3.746 3.549 3.560	

4.6 Lead Compound Identification

After the identification of binding interactions and binding affinities of data set, possible active compounds were chosen i.e. hits were identified in order to get a lead compound. All the ligands were checked for their potency using three criterions, i.e.; their binding interactions, binding energy and IC50 values. Eight compounds were found competing for the lead position. These include class of Dictyostatin (AA1 and AA3), Epothilones (AA22, AA23, QAA1, QAA2 and QAA3) and Discodermolide (AA4). Dictyostatins were rejected as they did not form ionic interactions with the protein. Epothilones proved to be a good class with low IC50 values and average numbers of all the three kinds of interactions but the binding affinity values of this class were somewhat high and when compared with Discodermolide, their binding interactions too are few. A careful review of literature already present for both compounds has also showed the high potency of both Discodermolides and Epothilones. Hence, Discodermolide is identified as most active or lead compound. It has low IC50 value, a good binding affinity and strong Hydrogen, Ionic and Hydrophobic interactions with the target protein than the rest of ligands. The structure of this ligand along with its IC50 value, binding energy and interactions is shown in the Table 4.11. From the table it is seen that the number of ionic, Hydrogen and hydrophobic interactions is 7, 14 and 32 respectively.

Table 4.11: lead compound with structure and binding interactions

Ligand	Ionic Bonding	Hydrogen Bond	Hydrophobic bonding	IC50 µM
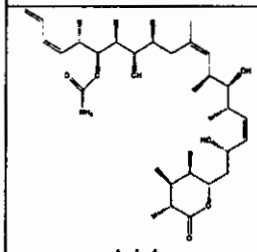 AA4	ARG369:N(3.748) GLY370:N(2.811) THR276:N(3.008) LEU230:N(3.313) HIS229:ND1(3.034) HIS229:NE2(3.882)	PRO274:O(2.328) LEU275:N(3.593) THR276:OG(3.959) THR276:N(3.193) THR276:O(3.732) LEU230:N(3.312) HIS229:ND1(3.223) ASP226:O(3.077) ASP226:N(3.756) ASP226:OD2(2.823) GLY225:O(3.210) ASP226:N(3.302) ASP226:O(3.834) ASP226:OD2(3.465)	ASP26:CG(3.879) VAL23:CG1(3.650) VAL23:CG1(3.689) ALA233:CA(3.876) ALA233:CB(3.728) PRO360:CB(3.696) PHE272:CE2(3.426) PHE272:CZ(3.958) PHE272:CE2(3.763) LEU371:CD1(3.688) LEU371:CD2(3.597) PRO274:CB(3.953) HIS229:CE1(3.815) HIS229:CE1(3.379) HIS229:CE1(3.982) LEU217:CD2(3.698) LEU230:CB(3.871) LEU217:CD2(3.705) LEU217:CG(3.561) LEU217:CD1(3.832) HIS229:CG(3.822) LEU219:CD2(3.575) LEU217:CD2(3.878) ASP226:CG(3.849) ASP226:CB(3.305) ASP226:CA(3.795) HIS229:CD2(3.691) LEU219:CD1(3.743) LEU219:CD2(3.572) LEU217:CD2(3.653) ARG278:CG(3.845) ARG278:CB(3.698)	0.0065

4.6.1 Binding Interactions of the Lead Compound

The figure 4.16 shows the interactions between the ligand and the protein and hence highlighting the amino acids of the protein pocket. It shows the distances also. The Oxygen of PRO274 with the distance 2.328, Nitrogen of LEU275 with 3.593, O of THR276 with 3.959, N of THR276 with 3.193, O of THR276 with 3.732, N of LEU230 with 3.312, N of HIS229 with 3.223, O of ASP226 with 3.077, N of ASP226 with 3.756, O of ASP226 with 2.823, O of GLY225 with 3.210, N of ASP226 with 3.302, O of ASP226 with 3.834 and again O of ASP226 with 3.465 in different conformations bind to Hydrogen of the lead for Hydrogen bondings.

The N of ARG369 with the distance 3.748, GLY370 with 2.811, THR276 with 3.008, LEU230 3.313, HIS229 with 3.034 and HIS229 with 3.882 bind with Oxygen of lead compound in different conformation to give ionic bonding.

For hydrophobic interactions the Carbon of lead compound bind in different conformations to the C of ASP26 with the distance 3.879, VAL23 with distances 3.650 and 3.689; ALA233 with 3.876, 3.728; PRO360 with 3.696; PHE272 with 3.426, 3.958, 3.763; LEU371 with 3.688 and 3.597; PRO274 with 3.953; HIS229 with 3.815, 3.379, 3.982, 3.822 and 3.691; LEU217 with 3.698, 3.705, 3.561, 3.832, 3.878 and 3.653; LEU230 with 3.871; LEU219 with 3.575, 3.743 and 3.572; ASP226 with 3.849, 3.305 and 3.795 and finally ARG278 with 3.845 and 3.698.

We based our comparison on the number of interactions formed with the target protein of the two compounds. As presented above, it is clearly seen that the number of interactions present in the lead compound are more as compared to the standard compounds. It will prove to be more potent than the already present drugs. Studies have also shown that Discodermolide proves to be more potent than Paclitaxel and its semi-synthetic analog, Docetaxel. So this research work verifies the work and authenticates it with experimental results.

Figure 4.16: Amino acid residues of active site of 1JFF bind with AA4 (Discodermolide)

4.7 Analogues of Lead Compound

The lead compound was analyzed in detail with respect to its structure and chemistry. Five analogs are suggested after the thorough examination. Table 4.12 shows the analogues of the lead compound with their IUPAC names obtained from ChemDraw software. The analogues have been made by the introduction or removal of various groups, or replacement of one group with another. In the first analogue, C-alkylation is performed where an alkyl group i.e., Methyl is introduced in the structure. This will increase the hydrophobic character of the compound. Amine formation is performed in the second analogue when a Carbonyl group is replaced with Amine group (NH_2) which increases hydrophilic character of the compound. This is because Amine group decreases the polarity and thus hydrophobicity is decreased. In the third analogue, again hydrophilicity is increased by hydroxylation. Alkene double bond has been replaced by 2 Hydroxyl groups on the two Carbons. Third analogue is Alcohol formation which again increases the hydrophilic character and decreases hydrophobicity. The carbonyl group is replaced by Hydroxyl (-OH) group in this case. Finally, ring opening is done in fifth and last analogue. This also increases hydrophilicity due to conversion of ring into straight chain and introduction of Hydroxyl groups on both ends.

Previously, multiple analogs have been made for the selected lead compound, i.e., Discodermolide. Four of them have already been used in this study.

Table 4.12: Analogues of the lead compound along the IUPAC names and structures

S. No.	Design technique	IUPAC Name	Structure of the Analogue
1.	C-alkylation	(3Z, 5S, 6S, 8R, 9S, 11Z, 13S, 14S, 15S, 16Z, 18S)-8, 18-dihydroxy-14-methoxy-5,7,9,11,13,15-hexamethyl-19-((2S,3R)-3,4,5-trimethyl-6-oxo-3,6-dihydro-2H-pyran-2-yl)nonadeca-1,3,11,16-tetraen-6-yl carbamate	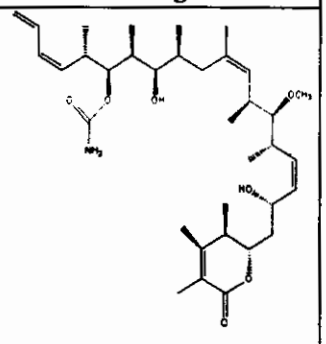
2.	Amine formation	(5R,6S)-6-((2S,3Z,5S,6S,7S,8Z,11S,12R,13S,14S,15S,16Z)-14-(aminomethoxy)-2,6,12-trihydroxy-5,7,9,11,13,15-hexamethylnonadeca-3,8,16,18-tetraenyl)-3,4,5-trimethyl-5,6-dihydropyran-2-one	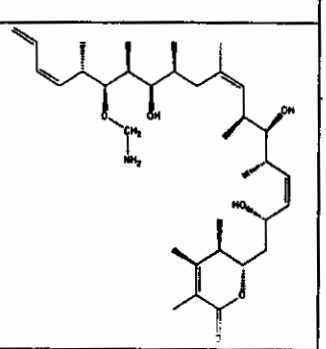
3.	Hydroxylation	(3Z,5S,6S,7S,8R,9S,11Z,13S,14S,15S,16Z,18S)-1,2,8,14,18-pentahydroxy-5,7,9,11,13,15-hexamethyl-19-((2S,3R)-3,4,5-trimethyl-6-oxo-3,6-dihydro-2H-pyran-2-yl)nonadeca-3,11,16-trien-6-yl carbamate	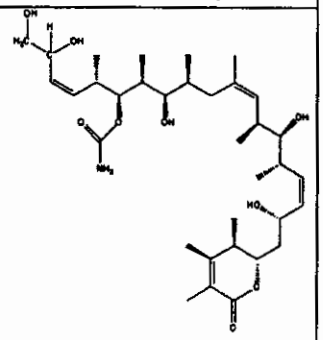
4.	Alcohol formation	(5R,6S)-3,4,5-trimethyl-6-((2S,3Z,5S,6S,7S,8Z,11S,12R,13S,14S,15S,16Z)-2,6,12,14-tetrahydroxy-5,7,9,11,13,15-hexamethylnonadeca-3,8,16,18-tetaenyl)-5,6 - dihydropyran-2-one	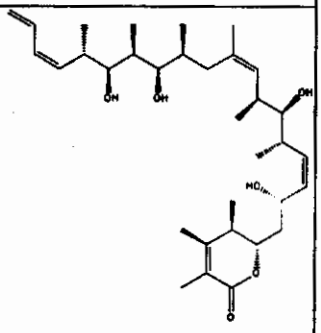

5.	Ring opening	(2Z,4R,5S,7S,8Z,10S,11S,12S,13Z,16S,17R,18S,19S,20S,21Z)-19-(carbamoyloxy)-5,7,11,17-tetrahydroxy-2,3,4,10,12,14,16,18,20-nonamethyltetracosa-2,8,13,21,23-pentaenoic acid	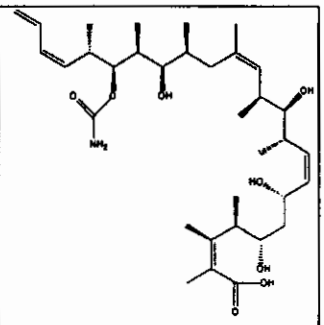

4.7.1 Docking and Interactions of Analogues with the Target Protein

Docking of the analogues has been performed for predicting the bound conformations and binding affinity of the analogues with the target protein. ADTools and AutoDock Vina are again used for the docking. Table 4.13 enlists all the Hydrogen, Ionic and Hydrophobic binding interactions of the analogs. The binding affinity (Energy) values are also included in the table. Figures 4.17-4.21 shows these interactions. On the basis of the number of interactions and low binding affinity values, analogs 2 and 3 are suggested for wet lab experiments and designing of new and highly potent anti-cancer drugs.

Table 4.13: binding interactions of analogs

S.No.	Ionic		Hydrogen		Hydrophobic		Energy Value Kcal/mol
	Bond	Distance	Bond	Distance	Bond	Distance	
Analog1	HIS229:ND1	3.11	HIS229:ND1	3.30	ALA233:CB	3.63	-10.2
	HIS229:NE2	3.51			ARG369:CB	3.87	
	ARG278:N	3.17			PHE272:CZ	3.78	
					PHE272:CE2	3.80	
					VAL23:CG1	3.49	
					LEU219:CD2	3.51	
					LEU219:CD2	3.97	
					GLY370:CA	3.79	
					HIS229:CE1	3.63	
					LEU217:CD2	3.81	
					LEU217:CD2	3.79	
					PRO360:CB	3.68	
					ALA233:CA	3.91	
					ALA233:CB	3.99	
					LEU217:CD2	3.62	
					LEU217:CD2	3.52	
					LEU217:CD2	3.58	
					LEU217:CD2	3.76	
Analog2	ARG278:N	3.78	PRO360:O	2.57	ALA233:CB	3.88	-11.3
	PRO360:O	3.48	PRO360:O	3.77	VAL23:CG1	3.53	
	ARG284:NH1	2.81	GLY370:N	3.25	VAL23:CG1	3.62	
	ASP26:OD1	2.99	GLY370:N	3.99	HIS229:CE1	3.63	
			LEU371:N	3.05	HIS229:CE1	3.99	
			LEU371:N	3.03	PHE272:CE2	3.74	
			ARG369:N	3.98	PHE272:CZ	3.78	
			THR276:OG1	3.45	GLN282:CB	3.65	
			ARG278:N	3.59	GLN282:CB	3.54	
			THR276:O	3.29	GLN282:CG	3.59	
			ARG278:O	2.88	GLN282:CG	3.99	
			SER277:O	2.80	PRO360:CB	3.70	
			GLU27:N	3.88	PRO360:CB	3.50	
			GLY370:O	2.81	LEU371:CD1	3.63	
			GLU27:N	3.38	PRO360:CB	3.42	
					GLU22:CB	3.82	
					VAL23:CG2	3.78	
					VAL23:CG1	3.46	
					HIS229:CE1	3.87	
					HIS229:CE1	3.61	
					ALA233:CB	3.60	
					ASP26:CG	3.76	
					PHE272:CZ	3.67	
					PHE272:CE1	3.91	
					PHE272:CE2	3.71	
					PHE272:CE2	3.70	
					LEU286:CD1	3.63	
					LEU371:CD2	3.72	
					VAL23:CA	3.73	
					PRO274:CB	3.84	
					PRO360:CB	3.79	
					LEU371:CB	3.18	
					LEU371:CB	3.78	
					GLY370:C	3.94	

					ARG284:CA	3.90	
Analog3	HIS229:NE2	3.52	GLY370:N	2.50	LEU219:CB	3.76	-10.5
	HIS229:NE2	3.56	HIS229:NE2	2.89	LEU219:CA	3.75	
	HIS229:ND1	3.95	THR276:O	3.01	LEU219:CD2	3.79	
	GLY370:N	3.22	THR276:O	3.85	LEU219:CD1	3.79	
	LYS218:N	3.23	LYS218:N	3.11	LEU275:CD1	3.76	
	LYS219:N	3.03	LEU219:N	2.76	GLU27:CB	3.72	
	GLY370:N	2.95	HIS229:NE2	3.53	GLU27:CG	3.76	
	HIS229:NE2	3.45	LYS218:O	3.77	PRO360:CB	3.89	
	HIS229:NE2	3.93	ARG278:N	3.53	PRO360:CB	3.53	
	GLY370:N	3.85	LEU371:N	3.83	PRO360:CB	3.98	
			PRO360:O	3.62	LEU217:CD2	3.52	
			ASP226:OD1	2.50	ALA233:CB	3.58	
			ASP226:OD2	3.03	ALA233:CA	3.81	
			GLY370:N	3.03	VAL23:CG1	3.50	
			HIS229:NE2	3.17	VAL23:CG2	3.86	
			HIS229:NE2	3.68	VAL23:CG1	3.47	
					VAL23:CG1	3.97	
					VAL23:CG1	3.70	
					PRO360:C	3.58	
					LEU217:CD1	3.83	
					LEU217:CG	3.72	
					PHE272:CE2	3.75	
					PHE272:CE2	3.65	
					PHE272:CZ	3.81	
					LEU275:CD1	3.65	
					GLU27:CD	3.85	
					LEU275:CD1	3.43	
					PHE272:CZ	3.21	
					PHE272:CE2	3.76	
					PRO360:CB	3.41	
					LEU217:CG	3.96	
					LEU217:CD2	3.83	
					GLY225:C	3.69	
					GLY225:CA	3.86	
					HIS229:CD2	3.67	
					ARG369:CB	3.72	
					LEU217:CD1	3.56	
					LEU219:CD1	3.69	
					ARG369:CB	3.65	
Analog4	ARG278:N	3.70	ARG278:N	3.50	PHE272:CE1	3.95	-10.8
	LYS372:N	3.78	SER277:O	2.73	PHE272:CE1	3.96	
			THR276:O	3.19	PRO360:CB	3.69	
			THR276:OG1	3.43	PRO360:CB	3.53	
			ARG278:O	2.89	PRO360:CB	3.64	
					LEU371:CD1	3.59	
					GLY370:C	3.95	
					GLN282:CB	3.59	
					GLN282:CB	3.55	
					GLN282:CG	3.59	
					PHE272:CE2	3.71	
					PHE272:CZ	3.77	
					ALA233:CB	3.81	
					HIS229:CE1	3.63	
					VAL23:CG1	3.54	
					VAL23:CG1	3.65	
					HIS229:CE1	3.95	

Analog5	HIS229:NE2	3.33	HIS229:NE2	2.78	PRO360:CB	3.92	-10.4
					LEU275:CD1	3.96	
					PHE272:CE2	3.81	
					PHE272:CE2	3.75	
					PHE83:CZ	3.66	
					ASP26:CG	3.97	
					ASP26:CG	3.45	
					LEU217:CD2	3.21	
					LEU217:CD2	3.74	
					LEU217:CD2	3.43	
					LEU217:CD2	3.41	
					LEU217:CD2	3.74	
					LEU217:CD2	3.82	
					LEU219:CD2	3.49	
					ASP226:CB	3.92	
					ASP226:CG	3.97	
					VAL23:CG1	3.52	
					LEU230:CA	3.95	
					LEU230:CB	3.53	
					ASP26:CG	3.59	
					GLU22:C	3.73	
					HIS229:CE1	3.26	

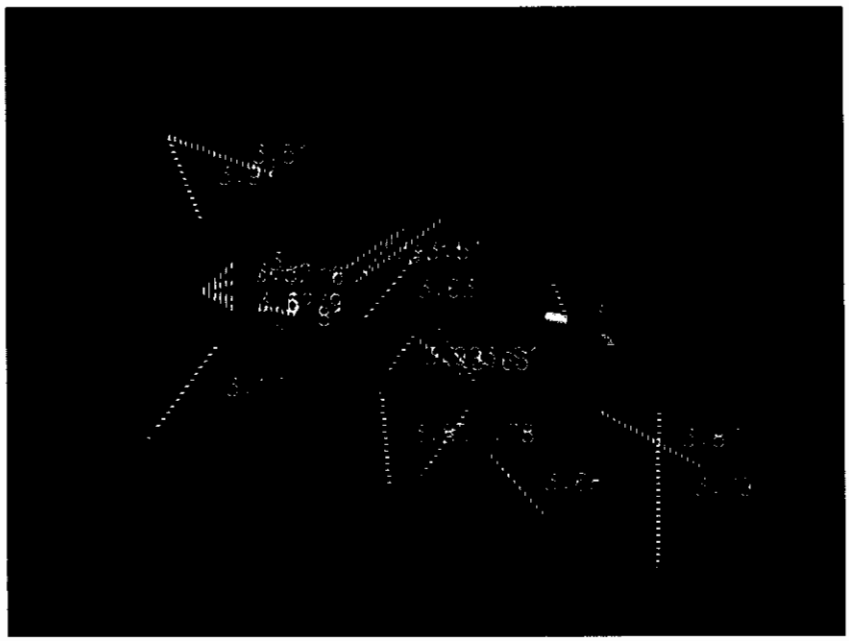

Figure 4.17: Amino acid residues of active site of 1JFF bind with Analog1

Figure 4.18: Amino acid residues of active site of 1JFF bind with Analog2

Figure 4.19: Amino acid residues of active site of 1JFF bind with Analog3

Figure 4.20: Amino acid residues of active site of 1JFF bind with Analog4

Figure 4.21: Amino acid residues of active site of 1JFF bind with Analog5

4.8 Quantitative Structure Activity Relationship

QSAR model was built for describing how some descriptors were directly or indirectly related to the biological activity i.e. pharmacokinetics of a compound. A set of descriptor was chosen and this set was then applied to data set. These descriptors were assumed to influence whether a given compound will succeed or fail in binding to the target protein. Set of 35 compounds from Epothilone class was selected as shown in Table 3.1b (Nicolaou *et al.,* 1998; Nicolaou *et al.,* 2003). A QSAR has been interpreted by calculating a number of steric and electronic parameters by the use of software HyperChem and ChemDraw. The descriptors included partition coefficient i.e. Log P and molar refractivity as steric parameter, total binding energy, heat of formation, E_{HOMO}, E_{LUMO} as electronic parameters. The calculated descriptor values are mentioned in Table 4.14.

Table 4.14: QSAR properties for the data set of Epothilone analogs

Name.	IC50(nm)	Log P	V_m	M_R	E_{HOMO}	E_{LUMO}	E_{TOTAL} (a.u.)
QAA1	0.17	7.97	1316.47	117.8	-0.08729	0.067429	-243.8106546
QAA2	0.1	9.42	1335	120.86	-0.07566	0.15107	-238.509712
QAA3	0.3	9.59	1303.46	106.86	-0.04977	0.343008	-237.5966199
QAA4	3.5	8.95	1391.71	123.25	-0.32919	0.027768	-276.1436725
QAA5	4.4	8.78	1419.82	127.07	-0.00584	0.327829	-234.6047294
QAA6	0.4	8.02	1334.42	111.8	-0.25162	0.057302	-226.7184387
QAA7	3.3	8.51	1342.2	111.86	-0.19677	0.039239	-226.6638357
QAA8	4.3	8.55	1308.37	104.74	-0.47717	0.109477	-266.7509747
QAA9	8.6	7.69	1332.65	110.9	-0.1585	0.207222	-227.758931
QAA10	>100	8.22	1206.4	100.06	-0.92438	0.446338	-208.6726324
QAA11	50	8.5	1245.06	104.81	-1.23205	0.249195	-214.1108297
QAA12	>100	8.82	1192.84	98.37	-2.25716	0.342582	-210.4922805
QAA13	>100	8.42	1130.5	93.62	-3.02348	0.454549	-190.3991595
QAA14	22	9.11	1237.13	106.27	-2.00038	0.193843	-204.7179312
QAA15	10	8.42	1139.23	93.62	-1.67737	0.238609	-207.4232134
QAA16	>100	8.8	1137.72	88.4	-1.15003	0.435998	-192.5212381
QAA17	>100	9.24	1170.57	94.57	-1.259	0.307397	-192.5330732
QAA18	>100	9.78	1174.03	88.63	-2.32766	0.272958	-190.3210082
QAA19	>100	8.48	1159.89	87.61	-1.18683	0.399041	-189.3521931
QAA20	>100	10.12	1075.32	91.84	-1.12822	0.408367	-186.7742468
QAA21	>100	8.22	1222.07	100.06	-1.1314	0.21563	-208.5752539
QAA22	>100	8.82	1208.07	98.37	-1.11485	0.317998	-206.3941324
QAA23	20	8.42	1145.88	93.62	-1.14081	0.117475	-195.3049305
QAA24	>100	8.42	1162.15	93.62	-1.09717	0.363469	-195.4524865
QAA25	>100	8.42	1156.79	93.62	-1.09481	0.314066	-195.5087785
QAA26	>100	8.53	1145.57	95.66	-1.01765	0.634453	-190.4258559
QAA27	>100	9.78	1190.53	88.63	-1.03725	0.301919	-197.2499313
QAA28	>100	8.48	1177.86	87.61	-0.97914	0.600187	-198.3632938
QAA29	>100	10.12	1103.31	91.84	-1.01681	0.499542	-190.2608195
QAA30	80	8.73	1255.62	103.06	-0.36032	0.504999	-230.7850265
QAA31	10	8.58	1269.18	104.79	-0.39156	0.214227	-230.9357222
QAA32	1.2	9.49	1282.17	100.16	-0.08017	0.097832	-224.4962765
QAA33	2	9.19	1296.47	107.84	-0.10249	0.039067	-235.6668179
QAA34	0.54	7.5	1256.65	109.75	-0.11704	0.096257	-243.2894645
QAA35	0.4	7.35	1270.2	111.84	-0.02465	0.094549	-238.4386605

The first step in the performance of QSAR was the calculation of QSAR equation. The activity parameter used in the QSAR study is IC-50 value.

IC-50 = 1.996176198672E+002 + 2.203086786851E-003*(Vm) + -1.431059919954E+000*(MR) + -1.049728513405E+001*(EHOMO) + 1.249550873462E+002*(ELUMO) + 2.207159171781E-001*(ETOTAL)

In the next step, statistical analysis of the data is performed. For a good QSAR equation, RSQ value must be high. RSQ indicates the high fitness of the data to calculated QSAR equation. This will facilitate much better predictions for new test data. RSQ value is adjusted to give a new value according to the data set. If there is a high difference in actual and adjusted, it means the overall prediction is weaker. The F statistics show the measure of strength of regression. The QSAR equation is not effective or good if the critical F is greater than F statistics. Table 4.15 shows the values for the above statistical parameters.

Next, correlation of descriptors with activity is found. LogP and Heat of formation values are not correlated with activity so these descriptors are discarded from the set of descriptors. Correlation value ranges from -1 to +1 through 0. -1 indicates ideal negative correlation. 0 as correlation value means no correlation at all and +1 means perfect positive correlation. The correlation value is best for seeing the tendency of relevance between descriptors and activity (IC-50). To be a good predictor the descriptor should contribute more than half, that is more than 50% to the activity. The values indicated as percentage contribution are the independent RSQ values of each descriptor if they were alone. It shows that Molar volume (V_m), Molar refractivity (MR), E_{LUMO} and

E_{TOTAL} proved to be good descriptors for the activity. The table 4.16 shows the values of correlation and the percentage contribution.

Next, correlation of descriptors with activity is found. LogP and Heat of formation values are not correlated with activity so these descriptors are discarded from the set of descriptors. Correlation value ranges from -1 to +1 through 0. -1 indicates ideal negative correlation. 0 as correlation value means no correlation at all and +1 means perfect positive correlation. The correlation value is best for seeing the tendency of relevance between descriptors and activity (IC-50). To be a good predictor the descriptor should contribute more than half, that is more than 50% to the activity. The values indicated as percentage contribution are the independent RSQ values of each descriptor if they were alone. It shows that Molar volume (V_m), Molar refractivity (MR), E_{LUMO} and E_{TOTAL} proved to be good descriptors for the activity. The table 4.16 shows the values of correlation and the percentage contribution.

Further a plot was generated for the training data that was generated by the QSAR equation. This shows the relationship between the actual IC-50 values and those predicted by the QSAR model. This will prove how much rightly the equation is fitting the data. Table 4.17 shows the actual IC-50 values and the predicted values alongside. Figure 4.22 shows the plot between the actual and predicted values.

Table 4.15: Statistical parameters and their values

SS_R	59051.40
SS_E	17851.42
SS_T	76902.83
RSQ	76.79 %
Adjusted RSQ	72.78 %
F statistics	19.19
Critical F	2.49

Table 4.16: Correlation of descriptors with activity and the percentage contribution of each descriptor to activity

V_m	-0.77	59.11 %
MR	-0.77	59.70 %
E_{HOMO}	-0.64	41.58 %
E_{LUMO}	0.77	59.05 %
E_{TOTAL}	0.77	59.41 %

Table 4.17: Actual and predicted IC-50 values

S. No.	Actual	Predicted
1	101	78.50
2	50	49.18
3	101	81.51
4	101	114.64
5	22	62.80
6	10	72.00
7	101	99.68
8	101	75.99
9	101	91.90
10	101	97.33
11	101	92.20
12	101	51.90
13	101	67.39
14	20	51.71
15	101	82.00
16	101	75.78
17	101	113.18
18	101	80.48
19	101	118.33
20	101	101.72
21	80	70.85
22	10	32.36
23	1.2	22.62
24	2	2.09
25	0.54	4.89
26	0.4	1.81
27	0.17	-10.53
28	0.1	-3.37
29	0.3	40.51
30	3.5	-27.72
31	4.4	10.15
32	0.4	2.33
33	3.3	-0.56
34	4.3	12.42
35	8.6	21.14

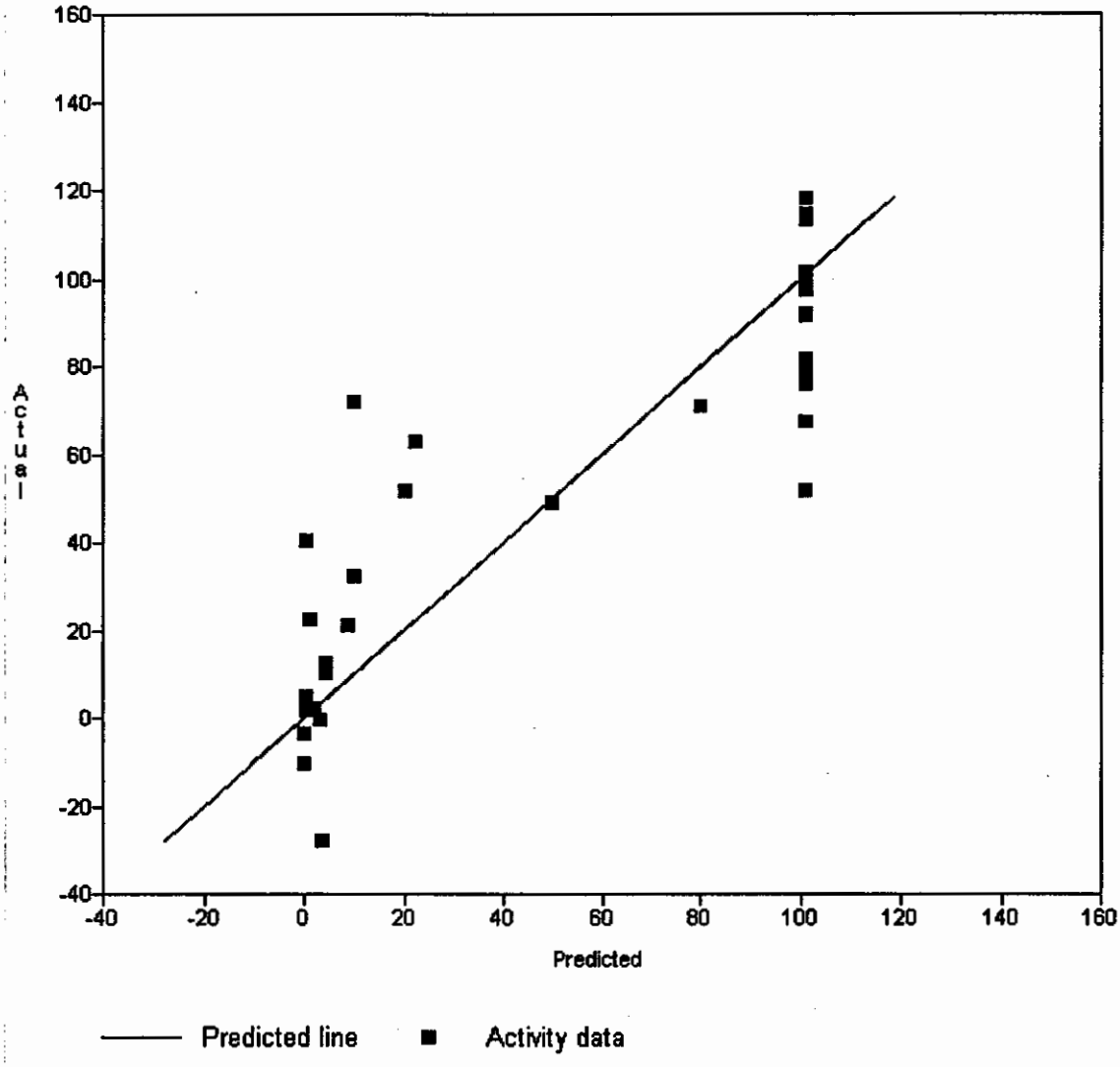

Figure 4.22: plot of actual and predicted IC-50 values

CONCLUSION & FUTURE ENHANCEMENTS

CONCLUSION & FUTURE ENHANCEMENTS

The present study shows that a set of compounds can be used to generate a good pharmacophore model with their activities ranging over several orders. The generated pharmacophore can be utilized effectively to predict the activity of a wide variety of chemical scaffolds. It can also be used as a 3D query for database searches. This helps in determining a variety of compounds that can prove as potent MSAAs. Secondly, it will also assist to assess how well newly designed compounds map onto the pharmacophore proceeding to undertake any further research including synthesis. Biological evaluation and optimization in designing or identifying compounds as potential MSAAs is also made possible by this pharmacophore study that showed the best model of MSAAs is made up of one Hydrogen bond donor, four Hydrogen bond acceptors and three hydrophobic features. The most active molecule in the training set fits the pharmacophore model perfectly with the highest scores.

Molecular docking was used as an advanced tool. Through the docking study, the important interactions between the potent inhibitors and the active site residues were determined. Using a combination of pharmacophore modeling, virtual screening, and molecular docking, putative novel MSAA is successfully identified, which can be further evaluated by in vitro and in vivo biological tests.

From the QSAR study, it is found that 35 analogs of Epothilone have prominent anticancer activity. Molar volume, molar refractivity, E_{HOMO}, E_{LUMO} and total energy parameters appeared to be the main governing physicochemical factors for the displayed

anti-cancer activities of these synthesized compounds. Such a QSAR evaluation would open future perspectives to use these compounds as new lead compounds in clinical trials.

With computational techniques like Molecular Dynamics (MD), the limitations imposed by the availability of crystal structures are overcome and a large number of different conformations can be generated. After docking of our dataset, now it is possible to perform MD simulations on this system. It will validate and optimize the Docked Complexes. QSAR descriptors can be investigated for other classes to propose specific descriptors important as MSAAs.

REFERENCES

REFERENCES

Auersperg N., Edelson M.I., Mok S.C., Johnson S.W., and Hamilton T.C., (1998) The biology of ovarian cancer, Semin. Oncol., 25, p. 281–304

Bast R. Jr., Boyer C.M., Jacobs I., Xu F.J., Wu S., Wiener J., Kohler M., and Berchuck A., (1993) Cell growth regulation in epithelial ovarian cancer, Cancer, 71, p. 1597–1601

Berchuck A., (1995) Biomarkers in the Ovary, J Cell Biochem., 23S, p. 223–226

Bergstralh D.T., and Ting J.P., (2006) Microtubule stabilizing agents: Their molecular signaling consequences and the potential for enhancement by drug combination, Cancer Treatment Reviews, 32, p. 166–179

Bharath E.N., Manjula S.N., Vijaychand A., (2011) *In Silico* Drug Designtool For Overcoming The Innovation Deficit In The Drug Discovery Process, International Journal of Pharmacy and Pharmaceutical Sciences, 3(2), p. 8-12

Bollag D.M., McQueney P.A., Zhu J., Hensens O., Koupal L., Liesch J., Goetz M., Lazarides E., and Woods C., (1995) Epothilones, a New Class of Microtubule-stabilizing Agents with a Taxol-like Mechanism of Action, Cancer Res., 55, p. 2325-2333

Cambridge MedChem Consulting, LigandScout 3.0 Review, (2009)

Ceccarelli S., Piarulli U., and Gennari C., (1999) Synthetic Studies on Sarcodictyins and Eleutherobin: Synthesis of Fully Functionalized Cyclization Precursors, Tetrahedron Letters, 40, p. 153-156

Chaudhry V., Rowinsky E.K., Sartorius S.E., Donehower R.C. and Cornblath D.R., (1994) Peripheral neuropathy from taxol and cisplatin combination chemotherapy: clinical and electrophysiological studies, Ann. Neurol., 35, p. 304–311

Checchi P.M., Nettles J.H., Zhou J., Snyder J.P., and Joshi H.C., (2003) Microtubule-interacting drugs for cancer treatment, Trends Pharmacol. Sci., 24, p. 361–365

Cheeseright T., Mackey M., Rose S., and Vinter A., (2006) Molecular field extrema as descriptors of biological activity: definition and validation, J. Chem. Inf. Model, 46, p. 665-676

Chou K.C., (2010) Graphic Rule for Drug Metabolism Systems, Curr. Drug Metab., 4, p. 369-378

Congreve M., Murray C.W., and Blundell T.L. (2005) Keynote review: Structural biology and drug discovery, DDT, 10(13), p. 895-907

Daly M., and Obrams G.I., (1998) Epidemiology and risk assessment for ovarian cancer, Semin. Oncol., 25, p. 255–264

Easton D.F., Bishop D.T., Ford D., and Crockford G.P., (1993) Genetic linkage analysis in familial breast and ovarian cancer: results from 214 families. The Breast Cancer Linkage Consortium, Am. J. Hum. Genet., 52, p. 678–701

Easton D.F., Ford D., and Bishop D.T., (1995) Breast and ovarian cancer incidence in BRCA1-mutation carriers. Breast Cancer Linkage Consortium, Am. J. Hum. Genet., 56, p. 265–271

Elie-Caille C., Severin F., Helenius J., Howard J., Muller D.J., and Hyman A.A., (2007) Straight GDP-Tubulin Protofilaments Form in the Presence of Taxol, Curr. Biol., 17, p. 1765–1770

Ewing T.J.A., and Kuntz I.D., (1997) Critical evaluation of search algorithms for automated molecular docking and database screening, J. Comput. Chem., 18, p. 1175-1189

George G.I., Chen T.T., Ojima I., and Vyas D.M., (1995) Taxane Anticancer Agents: Basic Science and Current Status. ACS Symposium Series. (Comstock, M.J., ed.) American Chemical Society, Washington, D.C.

Giannakakou P., Gussio R., Nogales E., Downing K.H., Zaharevitz D., Bollbuck B., Poy G., Sachett D., Nicolaou K.C. and Fojo T., (2000) A common pharmacophore for epothilone and taxanes: molecular basis for drug resistance conferred by tubulin mutations in human cancer cells, Proc. Natl. Acad. Sci. USA, 97, p. 2904–2909

Gonzalez-Diaz H., Duardo-Sanchez A., Ubeira F.M., Prado-Prado F., Perez-Montoto L.G., Concu R., Podda G., Shen B., (2010) Complex Networks Prediction of Drugs: ADMET, Anti-parasite Activity, Metabolizing Enzymes and Cardiotoxicity Proteome Biomarkers, Curr. Drug Metab., 4, p. 379-406

Guenard D., Gueritte-Voegelein F., Potier P., (1993) Taxol and taxotere: discovery, chemistry, and structure-activity relationships, Acc. Chem. Res., 26(4), p. 160–167

Gunasekera S.P., Gunasekera M., Longley R.E., Schulte G.K., (1990) Discodermolide: a new bioactive polyhydroxylated lactone from the marine sponge Discodermia dissolute, J. Org. Chem., 55(16), p. 4912–4915

Hamel E., (1996) Antimitotic Natural Products and Their Interactions with Tubulin, Medicinal Research Reviews, 16(2), p. 207-231

Hankinson S.E., Colditz G.A., Hunter D.J., Willett W.C., Stampfer M.J., Rosner B., Hennekens C.H., and Speizer F.E., (1995) A prospective study of reproductive factors and risk of epithelial ovarian cancer, Cancer, 76, p. 284–290

Hansch C., (1969) Quantitative approach to biochemical structure-activity relationships, Acc. Chem. Res., 2(8), p. 232–239

Harlow B.L., Cramer D.W., Bell D.A., and Welch W.R., (1992) Perineal exposure to talc and ovarian cancer risk, Obstet. Gynecol., 80, p. 19–26

Hartge P., Whittemore A.S., Itnyre J., McGowan L., and Cramer D., (1994) Rates and risks of ovarian cancer in subgroups of white women in the United States. The Collaborative Ovarian Cancer Group, Obstet. Gynecol., 84, p. 760–764

Hayden J.H., Bowser S.S., and Rieder C.L., (1990) Kinetochores capture astral microtubules during chromosome attachment to the mitotic spindle: direct visualization in live newt lung cells, J. Cell Biol., 111, p. 1039–1045

He L., Jagtap P.G., Kingston D.G.I., Shen H.-J., Orr G.A. and Horwitz S.B., (2000) A common pharmacophore for taxol and the epothilones based on the biological activity of a taxane molecule lacking a C-13 side chain, Biochemistry, 39, p. 3972–3978

Helzlsouer K.J., Alberg A.J., Norkus E.P., Morris J.S., Hoffman S.C., and Comstock G.W., (1996) Prospective study of serum micronutrients and ovarian cancer, J. Natl. Cancer Inst., 88, p. 32–37

Hileman B., (2006) Accounting for R&D, Many doubt the $800 million pharmaceutical price tag, Chemical Eng. News, 84, p. 50-51

http://www.pdb.org/pdb/explore.do?structureId=1ebz

Huang H.J., Yu H.W., Chen C.Y., Hsu C.H., Chen H.Y., Lee K.J., Tsai F.J., Chen C.Y.C., (2010) Current developments of computer-aided drug design, Journal of the Taiwan Institute of Chemical Engineers, 41(6), p. 623-635

Humphrey W., Dalke A., and Schulte K., (1996) VMD: Visual molecular dynamics, Journal of Molecular Graphics, 14(1), p. 33-38

Huzil J.T., Chen K., Kurgan L., and Tuszynski J.A., (2007) The Roles of β-Tubulin Mutations and Isotype Expression in Acquired Drug Resistance, Cancer Informatics, 3, p. 159–181

Hyams J. S., and Lloyd C. W., (1994) Microtubules, Wiley-Liss, New York

Hypercube, Inc., HyperChem® Release 7 for Windows®, (Jan 2002)

Isbrucker R.A., Cummins J., Pomponi S.A., Longley R.E., and Wright A.E., (2003) Tubulin polymerizing activity of dictyostatin-1, a polyketide of marine sponge origin, Biochemical Pharmacology, 66(1), p. 75-82

Jones G., Willett P., Glen R.C., Leach A.R., Taylor R., (1995) Molecular recognition of receptor sites using a genetic algorithm with a description of desolvation, J. Mol. Biol., 245(1), p. 43-53

Jordan M.A., Wilson L., (2004) Microtubules as a target for anticancer drugs, Nat. Rev. Cancer., 4, p. 253– 65

Kaku T., Ogawa S., Kawano Y., Ohishi Y., Kobayashi H., Hirakawa T., and Nakano H., (2003) Histological classification of ovarian cancer, Med. Electron Microsc, 36, p. 9–17

Kapetanovic I.M., (2008) Computer-aided drug discovery and development (CADDD): *In silico* chemico-biological approach, Chemico-Biological Interactions, 171, p. 165–176

Lee K.W. and Briggs J.M., (2001) Comparative molecular field analysis (CoMFA) study of epothilones–tubulin depolymerization inhibitors: pharmacophore development using 3D QSAR methods, J. Comput. Aid. Mol. Des., 15, p. 41–55

Li H., DeRosier D.J., Nicholson W.V., Nogales E., and Downing K.H., (2002) Microtubule structure at 8 Å resolution, Structure (Camb.), 10, p. 1317–1328

Lopez-Fanarraga M., Avila J., Guasch A., Coll M., and Zabala J.C., (2001) Review: postchaperonin tubulin folding cofactors and their role in microtubule dynamics, J. Struct. Biol., 135(2), p. 219–229

Lynch H.T., Casey M.J., Lynch J., White T.E., and Godwin A.K., (1998) Genetics and ovarian carcinoma, Semin. Oncol., 25, p. 265–280

Manetti F., Forli S., Maccari L., Corelli F., and Botta M., (2003) 3D QSAR studies of the interaction between β-tubulin and microtubule stabilizing antimitotic agents (MSAA). A combined pharmacophore generation and pseudoreceptor modeling approach applied to taxanes and epothilones, Il Farmaco, 58(5), p. 357-361

Mani S., Macapinlac M. Jr., Goel S., Verdier-Pinard D., Fojo T., Rothenberg M., Colevas D., (2004) The clinical development of new mitotic inhibitors that stabilize the microtubule, Anticancer Drugs, 15(6), p. 553–558

Martello L.A., LaMarche M.J., He L., Beauchamp T.J., Smith A.B. III, Horwitz S.B., (2001) The relationship between Taxol and (+)-discodermolide: synthetic analogs and modeling studies, Chemistry & Biology, 8, p. 843-855

Marti-Renom M.A., Stuart A.C., Fiser A., Sanchez R., Melo F., Sali A., (2000) Comparative Protein Structure Modeling of Genes and Genomes, Annu. Rev. Biophys. Biomol. Struct., 29, p. 291-325

Mccammon J.A., Gelin B.R., and Karplus M., (1977) Dynamics of Folded Proteins, Nature, 267, p. 585-590

Mills N., (2006) ChemDraw Ultra 10.0, J. Am. Chem. Soc., 128(41), p. 13649–13650

Mitchison T., and Kirschner M., (1984) Dynamic instability of microtubule growth, Nature, 312, p. 237–242

Mooberry S.L., Tien G., Hernandez A.H., Plubrukarn A., and Davidson B.S., (1999) Laulimalide and isolaulimalide, new paclitaxel-like microtubule stabilizing agents, Cancer Res., 59(3), p. 653–660

Morris G.M., Huey R., Lindstrom W., Sanner M.F., Belew R.K., Goodsell D.S., and Olson A.J., (2009) AutoDock4 and AutoDockTools4: Automated Docking with Selective Receptor Flexibility, Journal of Computational Chemistry, 30, p. 2785-2791

Murray C.W., Baxter C.A., and Frenkel A.D., (1999) The sensitivity of the results of molecular docking to induced fit effects: Application to thrombin, thermolysin and neuraminidase, J. Comput. Aided Mol. Des., 13, p. 547–562

Nicolaou K.C., Finlay M.R., Sacha Ninkovic S., King N.P., He Y., Li T., Sarabia F., Vourloumis D., (1998) Synthesis and biological properties of C12, 13-cyclopropylepothilone A and related epothilones, Chemistry & Biology, 5, p. 365-372

Nicolaou K.C., Sasmal P.K., Rassias G., Reddy M.V., Altmann K.H., Wartmann M., O'Brate A., Giannakakou P., (2003) Design, Synthesis, and Biological Properties of Highly Potent Epothilone B Analogues, Angew. Chem. Int., 42, p. 3515 –3520

Nicolaou K.C., VanDelft F., Hosokawa S., Kim S., Li T., Ohshima T., PfefferKorn J., Vourloumis D., Zu J.Y., Winssinger N., (1999) Analogs of Sarcodictyin and Eleutherobin. United States Patent. Patent # 5956718

Nogales E., and Wang H.W., (2006) Structural mechanisms underlying nucleotide-dependent self-assembly of tubulin and its relatives, Curr. Opin. Struct. Biol., 16(2), p. 221–229

Nogales E., Wolf S.G., Khan I.A., Luduena R.F., and Downing K.H., (1995) Structure of tubulin at 6.5 A and location of the taxol-binding site, Nature, 375, p. 424–427

Noureen N., Kalsoom S., and Rashid H., (2010) Ligand based pharmacophore modelling of anticancer histone deacetylase inhibitors, African Journal of Biotechnology, 9(25), p. 3923-3931

Ojima I., Chakravarty S., Inoue T., Lin S., He L., Horwitz S.B., Kuduk S.D. and Danishefsky S.J., (1999) A common pharmacophore for cytotoxic natural products that stabilize microtubules, Proc. Natl. Acad. Sci. USA, 96, p. 4256–4261

Parness J., and Horwitz, S.B. (1981) Taxol binds to polymerized tubulin in vitro, J. Cell Biol, 91, p. 479-487

Parvez T., (1992) Prevalence of Cancer in Different Hospitals of Lahore (Retrospective study), The Cancer Research, 1(2), p. 6-13

Paterson I., Gardner N.M., Poullenneca K.G., Wright A.E., (2007) Synthesis and biological evaluation of novel analogues of dictyostatin, Bioorganic & Medicinal Chemistry Letters, 17, p. 2443–2447

Paterson I., Menche D., Ha˚kansson A.E., Longstaff A., Wong D., Barasoain I., Buey R.M., Dı´az J.F., (2005) Design, synthesis and biological evaluation of novel, simplified analogues of laulimalide: modification of the side chain, Bioorganic & Medicinal Chemistry Letters, 15, p. 2243–2247

Perez-Montoto L.G., Prado-Prado F., Ubeira F.M., and Gonzalez-Diaz H., (2009) Study of Parasitic Infections, Cancer, and other Diseases with Mass-Spectrometry and Quantitative Proteome-Disease Relationships, Curr. Proteomics, 4, p. 246-261

Pettit G.R., and Cichacz Z.A., (1995) Isolation and structure of dictyostatin 1, US Patent No. 5,430,053

Prado-Prado F.J., Ubeira F.M., Borges F., and Gonzalez-Diaz H., (2009) Unified QSAR & network-based computational chemistry approach to antimicrobials. II. Multiple distance and triadic census analysis of antiparasitic drugs complex networks, J. Comput. Chem., 31, p. 164-173

Prado-Prado F.J., Uriarte E., Borges F., and Gonzalez-Diaz H., (2009) Multi-target spectral moments for QSAR and Complex Networks study of antibacterial drugs, Eur. J. Med. Chem., 44, p. 4516-4521

PricewaterhouseCoopers, "Pharma 2020: The vision – Which path will you take?" (2007) Available at http://www.pwc.com/pharma2020

Rarey M., Kramer B., Lengauer T., and Klebe G., (1996) A fast flexible docking method using an incremental construction algorithm, J. Mol. Biol., 261, p. 470–489

REFERENCES

Risch H.A., and Howe G.R., (1995) Pelvic inflammatory disease and the risk of epithelial ovarian cancer, Cancer Epidemiol Biomarkers Prev., 4, p. 447–451

Risinger A.L., and Mooberry S.L., (2010) Taccalonolides: Novel microtubule stabilizers with clinical potential, Cancer Letters, 291, p. 14-19

Risinger A.L., Giles F.J., and Mooberry S.L., (2009) Microtubule dynamics as a target in oncology, Cancer Treatment Reviews, 35, p. 255–261

Rossing M.A., Daling J.R., Weiss N.S., Moore D.E., and Self S.G., (1994) Ovarian tumors in a cohort of infertile women, N. Engl. J. Med., 331, p. 771–776

Rusan N.M., Fagerstrom C.J., Yvon A.M., and Wadsworth P., (2001) Cell cycle-dependent changes in microtubule dynamics in living cells expressing green fluorescent protein-alpha Tubulin, Mol. Biol. Cell, 12, p. 971– 80

Schrijvers D., Wanders J., Dirix L., Prove A., Vonck I., Oosterom A.V. and Kaye S., (1993) Coping with toxicities of docetaxel (taxotere), Ann. Oncol., 4, p. 610–611

Serov S.F., Scully R.E. and Sobin L.H., (1973) International Histologic Classification of Tumors. No. 9. Histological typing of Ovarian Tumors Geneva: World Health Organization.

Singer J.A., and William P., (1967) Purcell Relationships among Current Quantitative Structure–Activity Models, J. Med. Chem., 10, p. 1000-1002

Singh P., Rathinasamy K., Mohan R., and Panda D., (2008) Microtubule Assembly Dynamics: An Attractive Target for Anticancer Drugs, Life, 60(6), p. 368–375

Taft C.A., Da Silva V.B., and Da Silva C.H., (2008) Current Topics In Computer-Aided Drug Design, Journal Of Pharmaceutical Sciences, 97(3), p. 1089-1098

Tortolero-Luna G., and Mitchell M.F., (1995) The epidemiology of ovarian cancer, J. Cell Biochem., 59, p. 200–207

Trossini G.H.G., Guido R.V.C., Oliva G., Ferreira E.I., and Andricopulo A.D., (2009) Quantitative structure–activity relationships for a series of inhibitors of cruzain from *Trypanosoma cruzi*: Molecular modeling, CoMFA and CoMSIA studies, J. Mol. Graph. Model, 28, p. 3-11

Trott O., and Olson A.J., (2010) AutoDock Vina: Improving the Speed and Accuracy of Docking with a New Scoring Function, Efficient Optimization, and Multithreading, J. Comput. Chem., 31, p. 455–461

Wang H.W. and Nogales E. (2005) Nucleotide-dependent bending flexibility of tubulin regulates microtubule assembly, Nature, 435, p. 911–915

Wang M., Xia X., Kim Y., Hwang D., Jansen J.H., Botta M., Liotta D.C. and Snyder J.P., (1999) A unified and quantitative receptor model for the microtubule binding of paclitaxel and epothilone, Org. Lett. 1, p. 43–46

Wani M.C., Taylor H.L., Monroe E. Wall M.E., Coggon P., McPhail A.T., (1971) Plant antitumor agents. VI. Isolation and structure of taxol, a novel antileukemic and antitumor agent from Taxus brevifolia, J. Am. Chem. Soc., 93(9), p. 2325–2327

Wilson L., and Jordan M.A., (1994) Pharmacological probes of microtubule function in Microtubules (Hyams, J. g Lloyd, C., eds), p. 59-84, Wilev-Liss, Inc., NewYork

Wilson L., and Jordan M.A., (1995) Microtubule dynamics: taking aim at a moving target, Chemistry & Biology, 2, p. 569-573

Winkler J. and Axelson P.H., (1996) A model for the taxol (paclitaxel) / epothilone Pharmacophore, Bioorg. Med. Chem. Lett., 6, p. 2963–2966

Wu G.S., Robertson D.H., Brooks C.L. and Vieth M., (2003) Detailed Analysis of Grid-based Molecular Docking: A Case Study of CDOCKER—A CHARMM-based MD Docking Algorithm, J. Comput. Chem., 24, p. 1549-1562

Zhai Y., Kronebusch P.J., Simon P.M., and Borisy G.G., (1996) Microtubule dynamics at the G2/M transition: abrupt breakdown of cytoplasmic microtubules at nuclear envelope breakdown and implications for spindle morphogenesis, J. Cell Biol, 135, p. 201–214

Zhang D., Holmes W.F., Wu S., Soprano D.R., Soprano K.J., (2000) Retinoids and Ovarian Cancer, Journal Of Cellular Physiology, 185, p. 1–20

REFERENCES

Auersperg N., Edelson M.I., Mok S.C., Johnson S.W., and Hamilton T.C., (1998) The biology of ovarian cancer, Semin. Oncol., 25, p. 281–304

Bast R. Jr., Boyer C.M., Jacobs I., Xu F.J., Wu S., Wiener J., Kohler M., and Berchuck A., (1993) Cell growth regulation in epithelial ovarian cancer, Cancer, 71, p. 1597–1601

Berchuck A., (1995) Biomarkers in the Ovary, J Cell Biochem., 23S, p. 223–226

Bergstralh D.T., and Ting J.P., (2006) Microtubule stabilizing agents: Their molecular signaling consequences and the potential for enhancement by drug combination, Cancer Treatment Reviews, 32, p. 166–179

Bharath E.N., Manjula S.N., Vijaychand A., (2011) *In Silico* Drug Designtool For Overcoming The Innovation Deficit In The Drug Discovery Process, International Journal of Pharmacy and Pharmaceutical Sciences, 3(2), p. 8-12

Bollag D.M., McQueney P.A., Zhu J., Hensens O., Koupal L., Liesch J., Goetz M., Lazarides E., and Woods C., (1995) Epothilones, a New Class of Microtubule-stabilizing Agents with a Taxol-like Mechanism of Action, Cancer Res., 55, p. 2325-2333

Cambridge MedChem Consulting, LigandScout 3.0 Review, (2009)

Ceccarelli S., Piarulli U., and Gennari C., (1999) Synthetic Studies on Sarcodictyins and Eleutherobin: Synthesis of Fully Functionalized Cyclization Precursors, Tetrahedron Letters, 40, p. 153-156

Chaudhry V., Rowinsky E.K., Sartorius S.E., Donehower R.C. and Cornblath D.R., (1994) Peripheral neuropathy from taxol and cisplatin combination chemotherapy: clinical and electrophysiological studies, Ann. Neurol., 35, p. 304–311

Checchi P.M., Nettles J.H., Zhou J., Snyder J.P., and Joshi H.C., (2003) Microtubule-interacting drugs for cancer treatment, Trends Pharmacol. Sci., 24, p. 361–365

Cheeseright T., Mackey M., Rose S., and Vinter A., (2006) Molecular field extrema as descriptors of biological activity: definition and validation, J. Chem. Inf. Model, 46, p. 665-676

Chou K.C., (2010) Graphic Rule for Drug Metabolism Systems, Curr. Drug Metab., 4, p. 369-378

Congreve M., Murray C.W., and Blundell T.L. (2005) Keynote review: Structural biology and drug discovery, DDT, 10(13), p. 895-907

Daly M., and Obrams G.I., (1998) Epidemiology and risk assessment for ovarian cancer, Semin. Oncol., 25, p. 255–264

Easton D.F., Bishop D.T., Ford D., and Crockford G.P., (1993) Genetic linkage analysis in familial breast and ovarian cancer: results from 214 families. The Breast Cancer Linkage Consortium, Am. J. Hum. Genet., 52, p. 678–701

Easton D.F., Ford D., and Bishop D.T., (1995) Breast and ovarian cancer incidence in BRCA1-mutation carriers. Breast Cancer Linkage Consortium, Am. J. Hum. Genet., 56, p. 265–271

Elie-Caille C., Severin F., Helenius J., Howard J., Muller D.J., and Hyman A.A., (2007) Straight GDP-Tubulin Protofilaments Form in the Presence of Taxol, Curr. Biol., 17, p. 1765–1770

Ewing T.J.A., and Kuntz I.D., (1997) Critical evaluation of search algorithms for automated molecular docking and database screening, J. Comput. Chem., 18, p. 1175-1189

George G.I., Chen T.T., Ojima I., and Vyas D.M., (1995) Taxane Anticancer Agents: Basic Science and Current Status. ACS Symposium Series. (Comstock, M.J., ed.) American Chemical Society, Washington, D.C.

Giannakakou P., Gussio R., Nogales E., Downing K.H., Zaharevitz D., Bollbuck B., Poy G., Sachett D., Nicolaou K.C. and Fojo T., (2000) A common pharmacophore for epothilone and taxanes: molecular basis for drug resistance conferred by tubulin mutations in human cancer cells, Proc. Natl. Acad. Sci. USA, 97, p. 2904–2909

Gonzalez-Diaz H., Duardo-Sanchez A., Ubeira F.M., Prado-Prado F., Perez-Montoto L.G., Concu R., Podda G., Shen B., (2010) Complex Networks Prediction of Drugs: ADMET, Anti-parasite Activity, Metabolizing Enzymes and Cardiotoxicity Proteome Biomarkers, Curr. Drug Metab., 4, p. 379-406

Guenard D., Gueritte-Voegelein F., Potier P., (1993) Taxol and taxotere: discovery, chemistry, and structure-activity relationships, Acc. Chem. Res., 26(4), p. 160–167

Gunasekera S.P., Gunasekera M., Longley R.E., Schulte G.K., (1990) Discodermolide: a new bioactive polyhydroxylated lactone from the marine sponge Discodermia dissolute, J. Org. Chem., 55(16), p. 4912–4915

Hamel E., (1996) Antimitotic Natural Products and Their Interactions with Tubulin, Medicinal Research Reviews, 16(2), p. 207-231

Hankinson S.E., Colditz G.A., Hunter D.J., Willett W.C., Stampfer M.J., Rosner B., Hennekens C.H., and Speizer F.E., (1995) A prospective study of reproductive factors and risk of epithelial ovarian cancer, Cancer, 76, p. 284–290

Hansch C., (1969) Quantitative approach to biochemical structure-activity relationships, Acc. Chem. Res., 2(8), p. 232–239

Harlow B.L., Cramer D.W., Bell D.A., and Welch W.R., (1992) Perineal exposure to talc and ovarian cancer risk, Obstet. Gynecol., 80, p. 19–26

Hartge P., Whittemore A.S., Itnyre J., McGowan L., and Cramer D., (1994) Rates and risks of ovarian cancer in subgroups of white women in the United States. The Collaborative Ovarian Cancer Group, Obstet. Gynecol., 84, p. 760–764

Hayden J.H., Bowser S.S., and Rieder C.L., (1990) Kinetochores capture astral microtubules during chromosome attachment to the mitotic spindle: direct visualization in live newt lung cells, J. Cell Biol., 111, p. 1039–1045

He L., Jagtap P.G., Kingston D.G.I., Shen H.-J., Orr G.A. and Horwitz S.B., (2000) A common pharmacophore for taxol and the epothilones based on the biological activity of a taxane molecule lacking a C-13 side chain, Biochemistry, 39, p. 3972–3978

Helzlsouer K.J., Alberg A.J., Norkus E.P., Morris J.S., Hoffman S.C., and Comstock G.W., (1996) Prospective study of serum micronutrients and ovarian cancer, J. Natl. Cancer Inst., 88, p. 32–37

Hileman B., (2006) Accounting for R&D, Many doubt the $800 million pharmaceutical price tag, Chemical Eng. News, 84, p. 50-51

http://www.pdb.org/pdb/explore.do?structureId=1ebz

Huang H.J., Yu H.W., Chen C.Y., Hsu C.H., Chen H.Y., Lee K.J., Tsai F.J., Chen C.Y.C., (2010) Current developments of computer-aided drug design, Journal of the Taiwan Institute of Chemical Engineers, 41(6), p. 623-635

Humphrey W., Dalke A., and Schulte K., (1996) VMD: Visual molecular dynamics, Journal of Molecular Graphics, 14(1), p. 33-38

Huzil J.T., Chen K., Kurgan L., and Tuszynski J.A., (2007) The Roles of β-Tubulin Mutations and Isotype Expression in Acquired Drug Resistance, Cancer Informatics, 3, p. 159–181

Hyams J. S., and Lloyd C. W., (1994) Microtubules, Wiley-Liss, New York

Hypercube, Inc., HyperChem® Release 7 for Windows®, (Jan 2002)

Isbrucker R.A., Cummins J., Pomponi S.A., Longley R.E., and Wright A.E., (2003) Tubulin polymerizing activity of dictyostatin-1, a polyketide of marine sponge origin, Biochemical Pharmacology, 66(1), p. 75-82

Jones G., Willett P., Glen R.C., Leach A.R., Taylor R., (1995) Molecular recognition of receptor sites using a genetic algorithm with a description of desolvation, J. Mol. Biol., 245(1), p. 43-53

Jordan M.A., Wilson L., (2004) Microtubules as a target for anticancer drugs, Nat. Rev. Cancer., 4, p. 253– 65

Kaku T., Ogawa S., Kawano Y., Ohishi Y., Kobayashi H., Hirakawa T., and Nakano H., (2003) Histological classification of ovarian cancer, Med. Electron Microsc, 36, p. 9–17

Kapetanovic I.M., (2008) Computer-aided drug discovery and development (CADDD): *In silico* chemico-biological approach, Chemico-Biological Interactions, 171, p. 165–176

Lee K.W. and Briggs J.M., (2001) Comparative molecular field analysis (CoMFA) study of epothilones–tubulin depolymerization inhibitors: pharmacophore development using 3D QSAR methods, J. Comput. Aid. Mol. Des., 15, p. 41–55

Li H., DeRosier D.J., Nicholson W.V., Nogales E., and Downing K.H., (2002) Microtubule structure at 8 Å resolution, Structure (Camb.), 10, p. 1317–1328

Lopez-Fanarraga M., Avila J., Guasch A., Coll M., and Zabala J.C., (2001) Review: postchaperonin tubulin folding cofactors and their role in microtubule dynamics, J. Struct. Biol., 135(2), p. 219–229

Lynch H.T., Casey M.J., Lynch J., White T.E., and Godwin A.K., (1998) Genetics and ovarian carcinoma, Semin. Oncol., 25, p. 265–280

Manetti F., Forli S., Maccari L., Corelli F., and Botta M., (2003) 3D QSAR studies of the interaction between β-tubulin and microtubule stabilizing antimitotic agents (MSAA). A combined pharmacophore generation and pseudoreceptor modeling approach applied to taxanes and epothilones, Il Farmaco, 58(5), p. 357-361

Mani S., Macapinlac M. Jr., Goel S., Verdier-Pinard D., Fojo T., Rothenberg M., Colevas D., (2004) The clinical development of new mitotic inhibitors that stabilize the microtubule, Anticancer Drugs, 15(6), p. 553–558

Martello L.A., LaMarche M.J., He L., Beauchamp T.J., Smith A.B. III, Horwitz S.B., (2001) The relationship between Taxol and (+)-discodermolide: synthetic analogs and modeling studies, Chemistry & Biology, 8, p. 843-855

Marti-Renom M.A., Stuart A.C., Fiser A., Sanchez R., Melo F., Sali A., (2000) Comparative Protein Structure Modeling of Genes and Genomes, Annu. Rev. Biophys. Biomol. Struct., 29, p. 291-325

Mccammon J.A., Gelin B.R., and Karplus M., (1977) Dynamics of Folded Proteins, Nature, 267, p. 585-590

Mills N., (2006) ChemDraw Ultra 10.0, J. Am. Chem. Soc., 128(41), p. 13649–13650

Mitchison T., and Kirschner M., (1984) Dynamic instability of microtubule growth, Nature, 312, p. 237–242

Mooberry S.L., Tien G., Hernandez A.H., Plubrukarn A., and Davidson B.S., (1999) Laulimalide and isolaulimalide, new paclitaxel-like microtubule stabilizing agents, Cancer Res., 59(3), p. 653–660

Morris G.M., Huey R., Lindstrom W., Sanner M.F., Belew R.K., Goodsell D.S., and Olson A.J., (2009) AutoDock4 and AutoDockTools4: Automated Docking with Selective Receptor Flexibility, Journal of Computational Chemistry, 30, p. 2785-2791

Murray C.W., Baxter C.A., and Frenkel A.D., (1999) The sensitivity of the results of molecular docking to induced fit effects: Application to thrombin, thermolysin and neuraminidase, J. Comput. Aided Mol. Des., 13, p. 547–562

Nicolaou K.C., Finlay M.R., Sacha Ninkovic S., King N.P., He Y., Li T., Sarabia F., Vourloumis D., (1998) Synthesis and biological properties of C12, 13-cyclopropylepothilone A and related epothilones, Chemistry & Biology, 5, p. 365-372

Nicolaou K.C., Sasmal P.K., Rassias G., Reddy M.V., Altmann K.H., Wartmann M., O'Brate A., Giannakakou P., (2003) Design, Synthesis, and Biological Properties of Highly Potent Epothilone B Analogues, Angew. Chem. Int., 42, p. 3515 –3520

Nicolaou K.C., VanDelft F., Hosokawa S., Kim S., Li T., Ohshima T., PfefferKorn J., Vourloumis D., Zu J.Y., Winssinger N., (1999) Analogs of Sarcodictyin and Eleutherobin. United States Patent. Patent # 5956718

Nogales E., and Wang H.W., (2006) Structural mechanisms underlying nucleotide-dependent self-assembly of tubulin and its relatives, Curr. Opin. Struct. Biol., 16(2), p. 221–229

Nogales E., Wolf S.G., Khan I.A., Luduena R.F., and Downing K.H., (1995) Structure of tubulin at 6.5 A and location of the taxol-binding site, Nature, 375, p. 424–427

Noureen N., Kalsoom S., and Rashid H., (2010) Ligand based pharmacophore modelling of anticancer histone deacetylase inhibitors, African Journal of Biotechnology, 9(25), p. 3923-3931

Ojima I., Chakravarty S., Inoue T., Lin S., He L., Horwitz S.B., Kuduk S.D. and Danishefsky S.J., (1999) A common pharmacophore for cytotoxic natural products that stabilize microtubules, Proc. Natl. Acad. Sci. USA, 96, p. 4256–4261

Parness J., and Horwitz, S.B. (1981) Taxol binds to polymerized tubulin in vitro, J. Cell Biol, 91, p. 479-487

Parvez T., (1992) Prevalence of Cancer in Different Hospitals of Lahore (Retrospective study), The Cancer Research, 1(2), p. 6-13

Paterson I., Gardner N.M., Poullenneca K.G., Wright A.E., (2007) Synthesis and biological evaluation of novel analogues of dictyostatin, Bioorganic & Medicinal Chemistry Letters, 17, p. 2443–2447

Paterson I., Menche D., Ha˚kansson A.E., Longstaff A., Wong D., Barasoain I., Buey R.M., Dı´az J.F., (2005) Design, synthesis and biological evaluation of novel, simplified analogues of laulimalide: modification of the side chain, Bioorganic & Medicinal Chemistry Letters, 15, p. 2243–2247

Perez-Montoto L.G., Prado-Prado F., Ubeira F.M., and Gonzalez-Diaz H., (2009) Study of Parasitic Infections, Cancer, and other Diseases with Mass-Spectrometry and Quantitative Proteome-Disease Relationships, Curr. Proteomics, 4, p. 246-261

Pettit G.R., and Cichacz Z.A., (1995) Isolation and structure of dictyostatin 1, US Patent No. 5,430,053

Prado-Prado F.J., Ubeira F.M., Borges F., and Gonzalez-Diaz H., (2009) Unified QSAR & network-based computational chemistry approach to antimicrobials. II. Multiple distance and triadic census analysis of antiparasitic drugs complex networks, J. Comput. Chem., 31, p. 164-173

Prado-Prado F.J., Uriarte E., Borges F., and Gonzalez-Diaz H., (2009) Multi-target spectral moments for QSAR and Complex Networks study of antibacterial drugs, Eur. J. Med. Chem., 44, p. 4516-4521

PricewaterhouseCoopers, "Pharma 2020: The vision – Which path will you take?" (2007) Available at http://www.pwc.com/pharma2020

Rarey M., Kramer B., Lengauer T., and Klebe G., (1996) A fast flexible docking method using an incremental construction algorithm, J. Mol. Biol., 261, p. 470–489

REFERENCES

Risch H.A., and Howe G.R., (1995) Pelvic inflammatory disease and the risk of epithelial ovarian cancer, Cancer Epidemiol Biomarkers Prev., 4, p. 447–451

Risinger A.L., and Mooberry S.L., (2010) Taccalonolides: Novel microtubule stabilizers with clinical potential, Cancer Letters, 291, p. 14-19

Risinger A.L., Giles F.J., and Mooberry S.L., (2009) Microtubule dynamics as a target in oncology, Cancer Treatment Reviews, 35, p. 255–261

Rossing M.A., Daling J.R., Weiss N.S., Moore D.E., and Self S.G., (1994) Ovarian tumors in a cohort of infertile women, N. Engl. J. Med., 331, p. 771–776

Rusan N.M., Fagerstrom C.J., Yvon A.M., and Wadsworth P., (2001) Cell cycle-dependent changes in microtubule dynamics in living cells expressing green fluorescent protein-alpha Tubulin, Mol. Biol. Cell, 12, p. 971– 80

Schrijvers D., Wanders J., Dirix L., Prove A., Vonck I., Oosterom A.V. and Kaye S., (1993) Coping with toxicities of docetaxel (taxotere), Ann. Oncol., 4, p. 610–611

Serov S.F., Scully R.E. and Sobin L.H., (1973) International Histologic Classification of Tumors. No. 9. Histological typing of Ovarian Tumors Geneva: World Health Organization.

Singer J.A., and William P., (1967) Purcell Relationships among Current Quantitative Structure–Activity Models, J. Med. Chem., 10, p. 1000-1002

Singh P., Rathinasamy K., Mohan R., and Panda D., (2008) Microtubule Assembly Dynamics: An Attractive Target for Anticancer Drugs, Life, 60(6), p. 368–375

Taft C.A., Da Silva V.B., and Da Silva C.H., (2008) Current Topics In Computer-Aided Drug Design, Journal Of Pharmaceutical Sciences, 97(3), p. 1089-1098

Tortolero-Luna G., and Mitchell M.F., (1995) The epidemiology of ovarian cancer, J. Cell Biochem., 59, p. 200–207

Trossini G.H.G., Guido R.V.C., Oliva G., Ferreira E.I., and Andricopulo A.D., (2009) Quantitative structure–activity relationships for a series of inhibitors of cruzain from *Trypanosoma cruzi*: Molecular modeling, CoMFA and CoMSIA studies, J. Mol. Graph. Model, 28, p. 3-11

Trott O., and Olson A.J., (2010) AutoDock Vina: Improving the Speed and Accuracy of Docking with a New Scoring Function, Efficient Optimization, and Multithreading, J. Comput. Chem., 31, p. 455–461

Wang H.W. and Nogales E. (2005) Nucleotide-dependent bending flexibility of tubulin regulates microtubule assembly, Nature, 435, p. 911–915

Wang M., Xia X., Kim Y., Hwang D., Jansen J.H., Botta M., Liotta D.C. and Snyder J.P., (1999) A unified and quantitative receptor model for the microtubule binding of paclitaxel and epothilone, Org. Lett. 1, p. 43–46

Wani M.C., Taylor H.L., Monroe E. Wall M.E., Coggon P., McPhail A.T., (1971) Plant antitumor agents. VI. Isolation and structure of taxol, a novel antileukemic and antitumor agent from Taxus brevifolia, J. Am. Chem. Soc., 93(9), p. 2325–2327

Wilson L., and Jordan M.A., (1994) Pharmacological probes of microtubule function in Microtubules (Hyams, J. g Lloyd, C., eds), p. 59-84, Wilev-Liss, Inc., NewYork

Wilson L., and Jordan M.A., (1995) Microtubule dynamics: taking aim at a moving target, Chemistry & Biology, 2, p. 569-573

Winkler J. and Axelson P.H., (1996) A model for the taxol (paclitaxel) / epothilone Pharmacophore, Bioorg. Med. Chem. Lett., 6, p. 2963–2966

Wu G.S., Robertson D.H., Brooks C.L. and Vieth M., (2003) Detailed Analysis of Grid-based Molecular Docking: A Case Study of CDOCKER—A CHARMM-based MD Docking Algorithm, J. Comput. Chem., 24, p. 1549-1562

Zhai Y., Kronebusch P.J., Simon P.M., and Borisy G.G., (1996) Microtubule dynamics at the G2/M transition: abrupt breakdown of cytoplasmic microtubules at nuclear envelope breakdown and implications for spindle morphogenesis, J. Cell Biol, 135, p. 201–214

Zhang D., Holmes W.F., Wu S., Soprano D.R., Soprano K.J., (2000) Retinoids and Ovarian Cancer, Journal Of Cellular Physiology, 185, p. 1–20